Development of waste heat recovery systems for mobile heavy duty applications

Thomas Cauwet

Master Thesis in Vehicle Engineering

Department of Aeronautical and Vehicle Engineering
KTH Royal Institute of Technology

TRITA-AVE 2013:53
ISSN 1651-7660

Postal address	***Visiting Address***	***Telephone***	***Telefax***	***Internet***
KTH	Teknikringen 8	+46 8 790 6000	+46 8 790 6500	www.kth.se
Vehicle Dynamics	Stockholm			
SE-100 44 Stockholm, Sweden				

Acknowledgments

I am grateful to my thesis supervisors, Thomas Reiche at Volvo and Lars Drugge at KTH for their guidance and support in this work.

A special thanks to Thomas Reiche, my thesis supervisor within Volvo AT&R who has contributed a lot in this work. I thank him for his wellbeing: always positive and ready to find solutions. He has always encouraged me a lot. I also thank Vincent Grelet for his knowledge, his support and his interest in this research project.

I would like to thank a lot of Volvo members that were implicated in the waste heat recovery system design. More precisely, the cooling system modeling and development team and in particular Peter Gullberg and Christoffer Bäckvall, AT&R's people working on electric and hybrid powertrain concepts and in particular Hellal Benzaoui.

Special thanks to all the AT&R team and more especially people with whom I shared the office: Romain, Vincent, Flavien, Guillaume and Hocéane.

Finally, I would like to thank Caroline for her support every day, all my KTH friends with a special thanks to Sarah, Vincent, Aubry, Quentin and Caroline and all the KTH professors who have contributed a lot to make this year and a half at KTH a very successful and rewarding experience.

Abstract

The focus of today's automotive industry is to reduce emissions and fuel consumption of all vehicles. Concentrating on the truck industry, the last 20 years have focused largely on cutting emissions of particulate matter and nitrogen oxides. For the future, attention will be focused on fuel consumption and emissions of carbon dioxide. Waste heat recovery appears to be a very promising concept for fuel economy on long haul heavy duty Diesel trucks.

After a general introduction on the concept of waste heat recovery and the Rankine cycle, this thesis work shows how to model and calibrate a cooling system circuit for a heavy duty Diesel engine equipped with a waste heat recovery system. Then an overview of the current transmission systems that are suitable to transfer energy from the waste heat recovery expander to the engine shaft is presented. For all transmission architectures, input speed range, speed ratio range, transmission efficiency as well as weight and size are detailed and compared to each other. Finally, these systems are modeled and integrated to a complete vehicle Simulink simulation platform and simulations are run on two highway driving cycles. Resulting average recovered powers and fuel consumptions are compared and the analysis finally shows that a gear train transmission has the best performance for this kind of driving cycle.

Contents

List of tables

List of figures

Nomenclature

A_{rad}	Radiator area	m^2
CAC	Charge Air Cooler	-
C_{fan}	Fan power factor	m^5
C_{flow}	Fan flow factor	m^3
$c_{p_{air}}$	Air specific heat capacity	$J.kg^{-1}.K^{-1}$
$c_{p_{exhaust}}$	Exhaust gases specific heat capacity	$J.kg^{-1}.K^{-1}$
$c_{p_{fluid}}$	Fluid (air or coolant) specific heat capacity	$J.kg^{-1}.K^{-1}$
EGR	Exhaust Gas Recirculation	-
ε	Power ratio	-
h_{air}	Air specific enthalpy	$J.kg^{-1}$
$h_{exhaust}$	Exhaust gases specific enthalpy	$J.kg^{-1}$
H_V	Fuel lower heating value	$J.kg^{-1}$
i_{gear}	Gear ratio	-
LT	Low Temperature	-
$\dot{m}_{air}$	Air mass flow	$kg.s^{-1}$
$\dot{m}_{charge\ air}$	Charge air mass flow	$kg.s^{-1}$
$\dot{m}_{exhaust}$	Exhaust gases mass flow	$kg.s^{-1}$
$\dot{m}_{fluid}$	Fluid (air or coolant) mass flow	$kg.s^{-1}$
$\dot{m}_{forced}$	Forced air mass flow	$kg.s^{-1}$
$\dot{m}_{fuel}$	Fuel mass flow	$kg.s^{-1}$
$\dot{m}_{natural}$	Natural air mass flow	$kg.s^{-1}$
n_{eng}	Engine rotational speed	rpm
n_{fan}	Fan rotational speed	rpm
η	Component efficiency	-
η_{mech}	Mechanical efficiency	-
η_{elec}	Electrical efficiency	-
η_{engine}	Engine efficiency	-

$\eta_{planetary}$	Planetary gear train efficiency	-
P_{brake}	Engine brake power	W
P_{mech}	Mechanical power	W
P_{elec}	Electrical power	W
P_{in}	Input power	W
P_{out}	Output power	W
ρ_{air}	Air density	$kg.m^{-3}$
$\dot{Q}_{CAC}$	Charge air cooler heat transfer rate	W
$\dot{Q}_{coolant}$	Coolant heat transfer rate	W
$\dot{Q}_{EGR}$	EGR gases heat transfer rate	W
$\dot{Q}_{exhaust}$	Exhaust gases heat transfer rate	W
$\dot{Q}_{fuel}$	Fuel heat transfer rate	W
$\dot{Q}_{miscellaneous}$	Miscellaneous (radiations, losses…) equivalent heat transfer rate	W
$\dot{Q}_{oil}$	Oil heat transfer rate	W
r	Fan speed ratio	-
R	Ring gear radius	m
R_{in}	Input gear radius	m
R_{out}	Output gear radius	m
r_{speed}	Speed ratio	-
S	Sun gear radius	m
SR	Speed ratio	-
T_{air}	Air temperature	K
T_{eng}	Engine torque	Nm
$T_{exhaust}$	Exhaust temperature	K
T_{exp}	Expander torque	Nm
T_{fluid}	Fluid temperature	K
T_{in}	Input torque	Nm
T_{m_1}	Generator/motor 1 torque	Nm
T_{out}	Output torque	Nm
T_R	Ring gear torque	Nm
τ	Time constant	s

$v_{vehicle}$	Vehicle speed	m.s^{-1}
ω_{eng}	Engine rotational speed	rad. s^{-1}
ω_{exp}	Expander rotational speed	rad. s^{-1}
ω_{in}	Input shaft rotational speed	rad. s^{-1}
ω_{m_1}	Generator/motor 1 rotational speed	rad. s^{-1}
ω_{out}	Output shaft rotational speed	rad. s^{-1}
ω_R	Ring gear rotational speed	rad. s^{-1}

Chapter 1: Introduction

1.1. General background

On-road transports account for the biggest part of inland freight transports and tend to increase as seen in Figure 1. On the other hand, fuel prices are also increasing pushing further more truck manufacturers to develop solutions to reduce the fuel consumption.

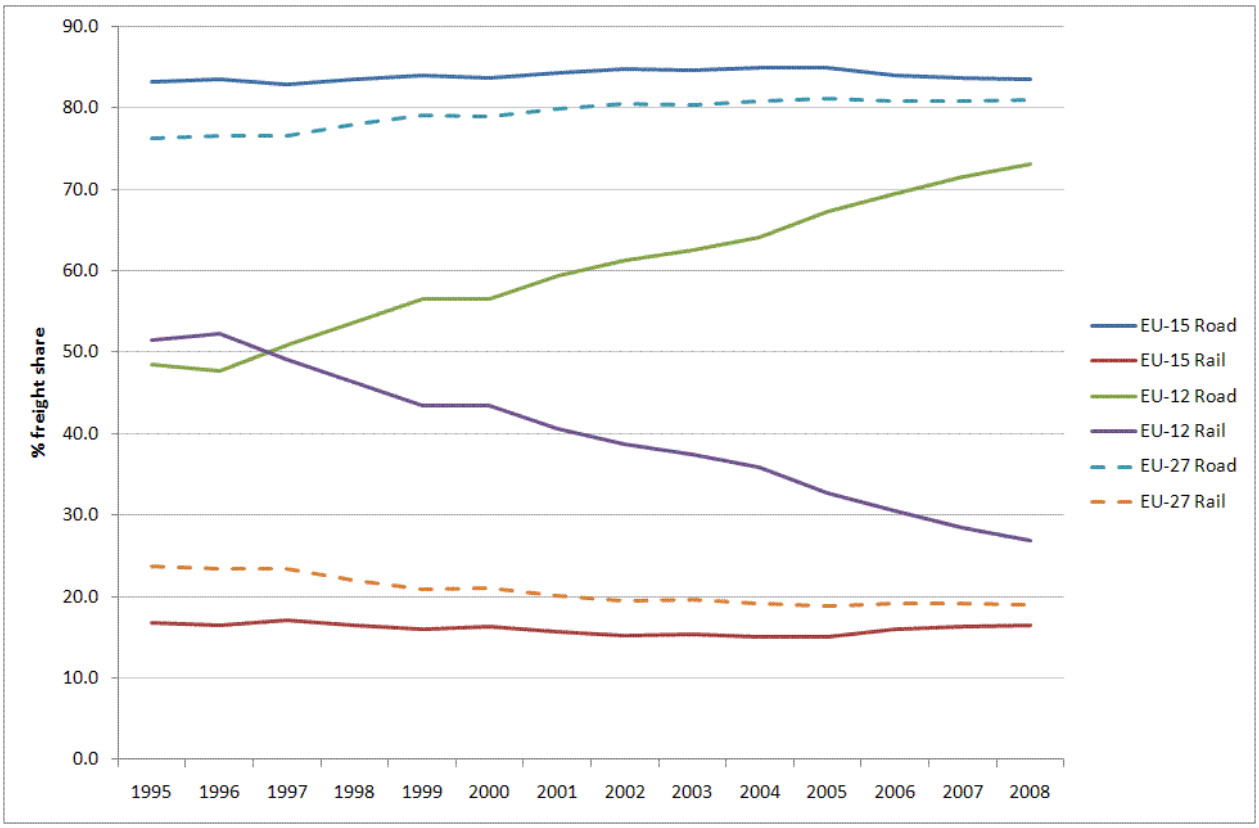

Figure 1: Percentage share of land freight transport between road and rail transport mode for EU12, EU15 and combined EU27 [1]

Hybrid powertrains are a possible solution to reduce fuel consumption in applications where the Diesel engine often operates in transient modes and at part load. Adding electric motors enables Diesel engines to be downsized and run on better operating conditions, thus increasing engine efficiency and reducing the fuel consumption. This is essentially the case for distribution, refuse trucks or buses. For long haul trucks, those conditions do not happen as often as for distribution trucks. The cost of a hybrid system is then too large compared to the expected gain in fuel consumption and these systems suffer from a lack of autonomy when large amounts of power are needed. The strategy developed for long haul trucks to improve the powertrain efficiency is thus waste heat recovery. Although waste heat recovery can be

applied to any type of on-road vehicles, the most attractive applications are the long haul heavy duty Diesel trucks because the engine load and speed are more stable over large period of operation and high mileages is accumulated as seen in Figure 2. As stable operating conditions give the best fuel saving performances, gains in fuel consumption will be sufficient to recover the added cost in a short period of time.

In addition to the reduction in fuel consumption and increase in profits for customers, waste heat recovery also reduces specific pollutant emissions and CO_2 emissions, which is likely to be the next combustion product to be regulated.

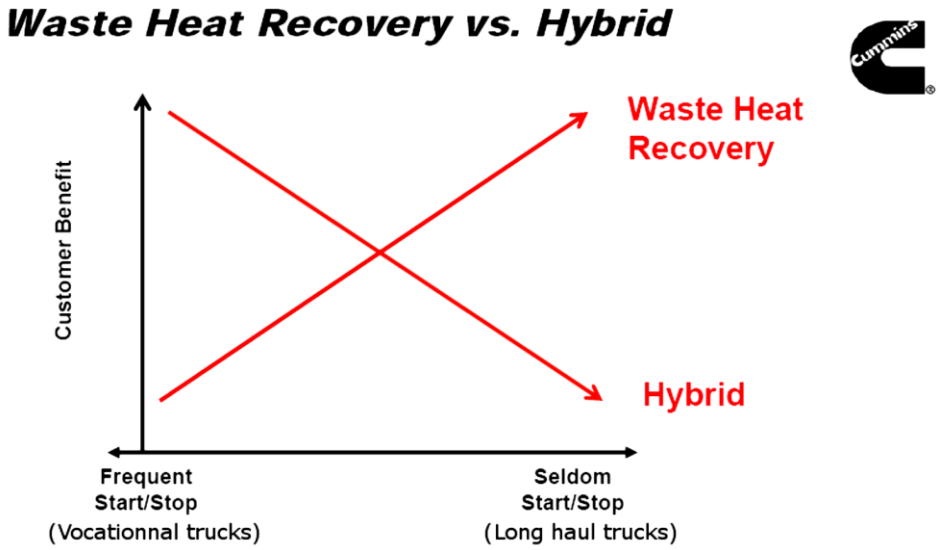

Figure 2: Identified applications for hybrid and waste heat recovery systems. Strategy from the engine manufacturer Cummins

1.1.1. Waste heat from heavy duty Diesel engines

Recent developments in Diesel engines have brought it to a good efficiency (40-42%) and low emission levels regarding particles and NO_x to comply with the more stringent regulations. However, part of the energy brought from the fuel is still dissipated as heat through the cooling system and the exhaust pipes and after treatment system. Waste heat can then be potentially recovered to improve engine efficiency and fuel consumption.

A comprehensive energy flow diagram for a typical turbo charged heavy duty Diesel engine with a high pressure EGR loop is presented in Figure 3 where $\dot{m}$ and $\dot{Q}$ are respectively mass flow and heat transfer rates, P denotes the power, h is the specific enthalpy and H_V is the lower heating value of the fuel. The subscript c stands for coolant.

The energy balance of a typical turbo charged heavy duty Diesel engine with high pressure EGR can be approximated as:

$$\dot{m}_{fuel} * H_V + \dot{m}_{air} * h_{air} = P_{brake} + \dot{m}_{exhaust} * h_{exhaust} + \dot{Q}_{coolant} + \dot{Q}_{CAC} + \dot{Q}_{EGR} \qquad \textbf{1-1}$$

The last four terms of the right hand side of the equation represent waste heat.

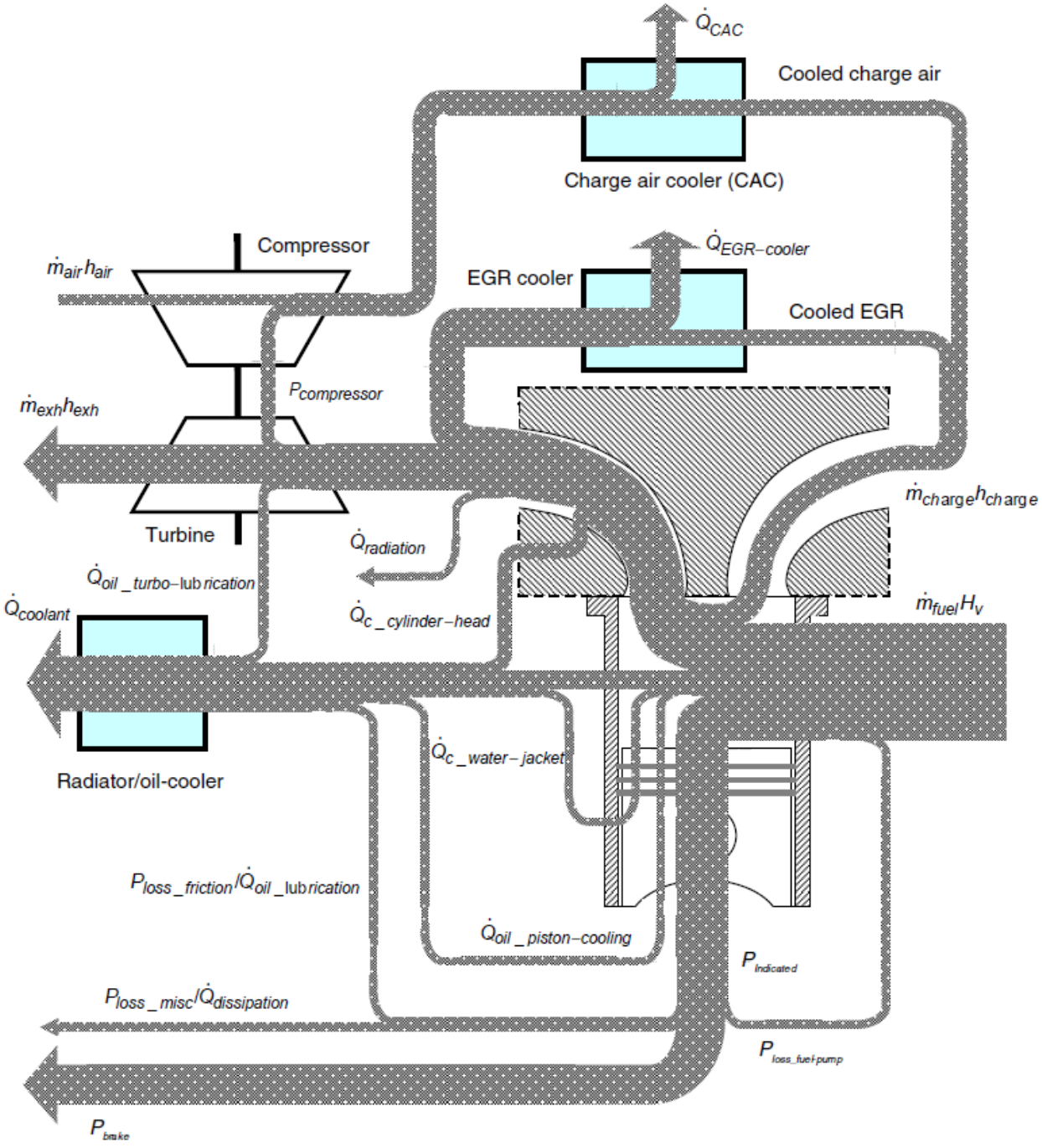

Figure 3: Energy flow diagram for a typical turbo charged heavy duty Diesel engine with high pressure EGR [2]

Figure 4 shows the balance of energy coming from fuel combustion in engine cylinders for a VT-NA MD13 500 hp US10 engine at 1285 rpm and 50% load.

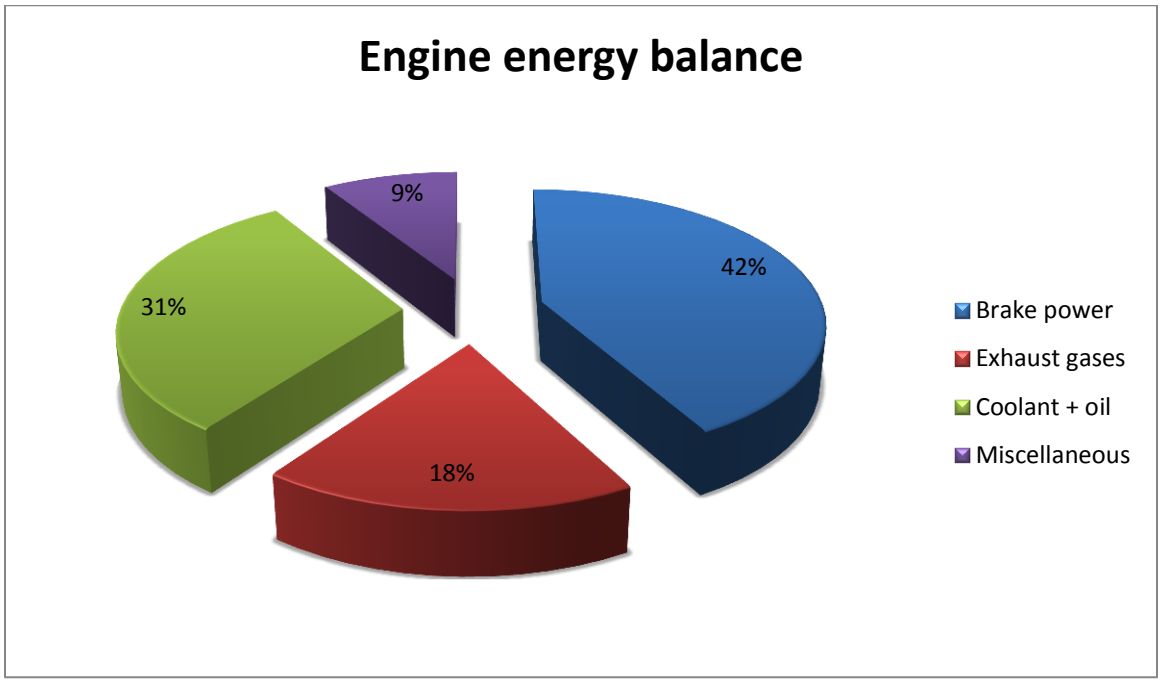

Figure 4: Typical energy balance of a VT-NA MD13 500 hp US10 engine at 1285 rpm and 50% load

1.1.2. Organic Rankine cycle

The Rankine cycle is an idealized thermodynamic cycle of a heat engine converting heat into mechanical power. One of the well-known examples of Rankine cycles is the steam engine developed during the industrial revolution. Nowadays, Rankine cycles are used to generate about 90% of electricity in the world.

Waste heat recovery systems based on the Rankine cycle are usually composed of a pump, one or several boilers, an expansion machine and a condenser. The ideal thermodynamic cycle that describe the heat to power conversion is depicted in the T-s diagram in Figure 5. The pump pressurizes the fluid (usually at liquid state) (transformation 1-2) before it evaporates at constant pressure level in a boiler in contact with a hot source like exhaust gases or EGR gases (transformation 2-3). The fluid is then superheated until a certain temperature in contact to the same or another hot source (transformation 3-3'). Then the superheated vapor expands in an expander such as a turbine or a piston machine until it reaches a lower pressure level (transformation 3'-4'). The expansion converts recovered heat into mechanical work. Finally, the fluid is brought back to its initial state in the condenser in contact with a cold source like coolant fluid or ambient air (transformation 4'-1). Typical layouts of devices used to convert heat to power are shown in Figure 6.

Since temperatures of waste heat rejected from heavy duty Diesel engines are of low and moderate levels, maximum efficiency and power output are obtained using an organic fluid like methanol, ethanol, refrigerant, etc. or fluid mixtures instead of water as working fluid. This is due to a lower temperature difference between waste heat and the working fluid.

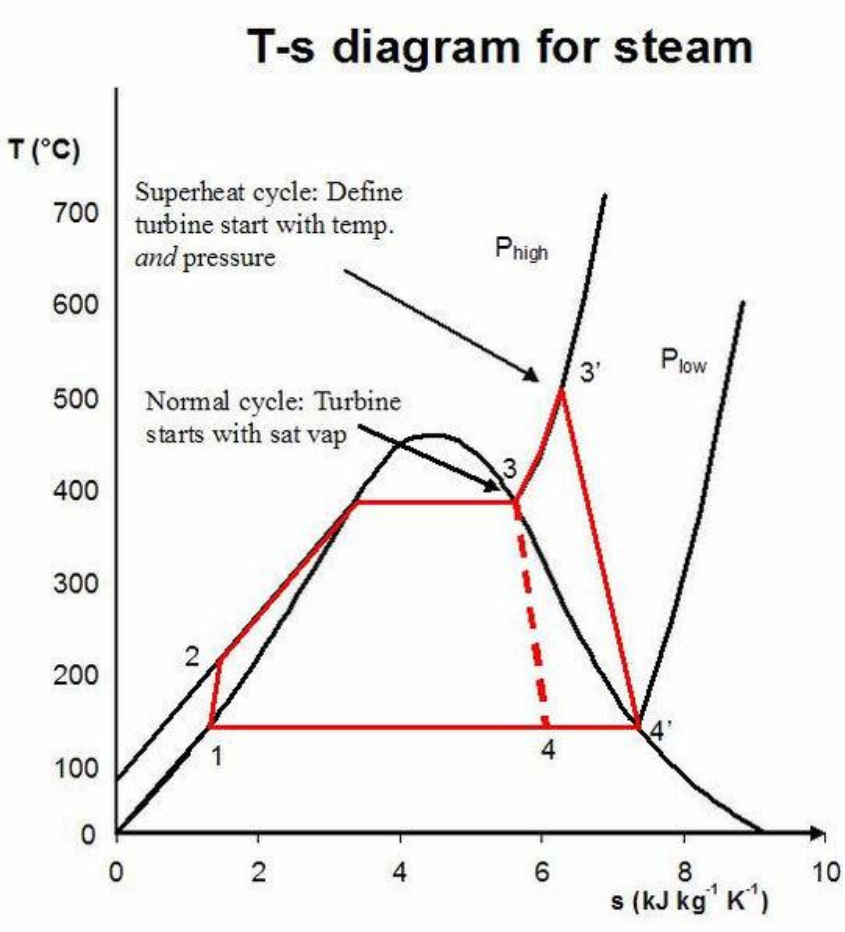

Figure 5: Rankine cycle T-s diagram with superheat [3]

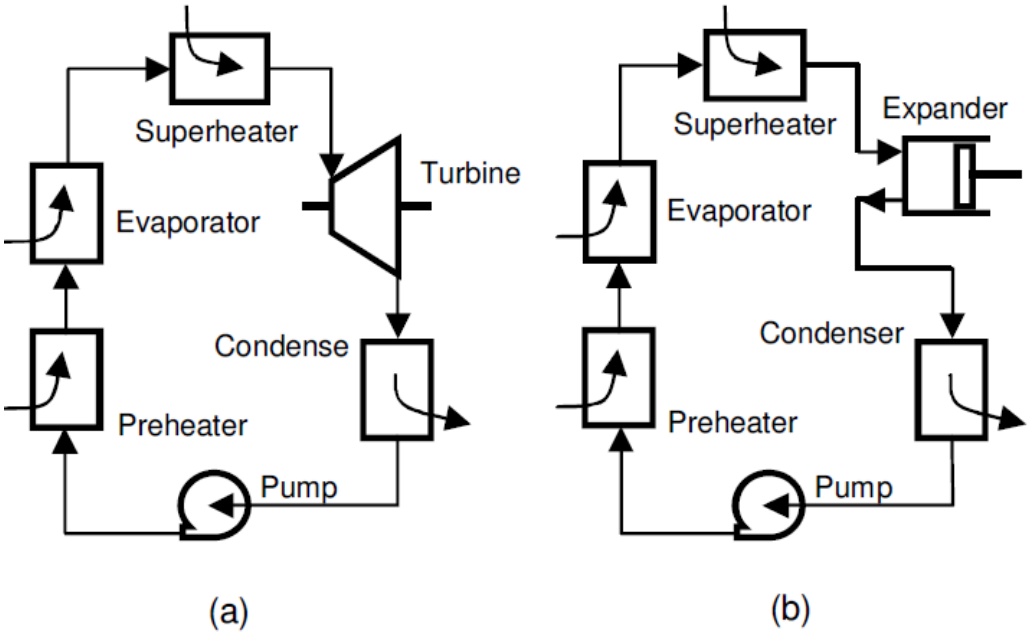

Figure 6: Turbine (a) and reciprocating (b) organic Rankine cycle waste heat recovery systems [2]

1.1.3. Simulation platform

The simulation platform used to implement models and simulate is called GSP that stands for Global Simulation Platform. It is a simulation tool based on Matlab-Simulink to evaluate fuel consumption and performances of different vehicle concepts.

As shown in Figure 7, GSP is comprised of three main models that interact between each other:

- A road model that imposes external conditions like ambient temperature and pressure and road characteristics like elevation, inclination, maximum allowed speed, stops, etc. to the driver and vehicle model.
- A driver model that defines how the driver behaves depending on road characteristics like its abilities to anticipate decelerations and stops, gearshift strategies, over speeding, etc.

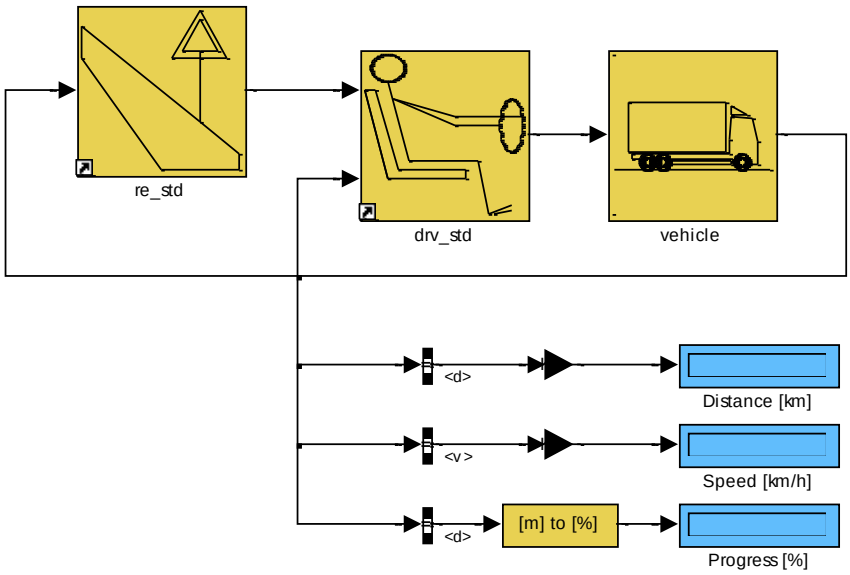

Figure 7: Global Simulation Platform – Model overview

- A complete vehicle model (see Figure 8) that contains the modeled physical components of the vehicle. The basic principle for energy flow is that it is accumulated until the last component, in which the differential equation for the system is solved. In the mechanical domain, this means that torques and inertias are accumulated downstream and angular speed integrated and sent upstream. The integration will be performed in the last component [4].

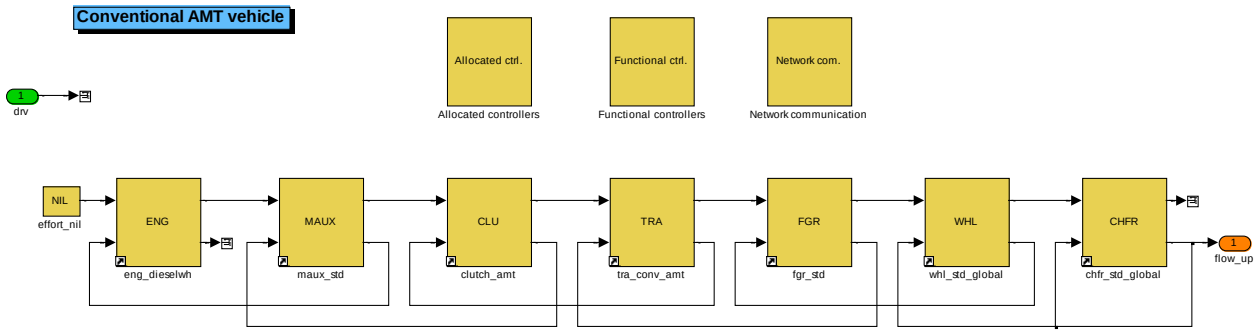

Figure 8: Global Simulation Platform - Vehicle model

This simulation platform provides accurate and fast results when comparison in terms of vehicle performances and fuel consumption are needed. The main drawback is that only mechanical (speed, torque) or electrical (current, voltage) quantities are at stake and output, there is nothing concerning thermodynamic quantities like pressures, temperatures, flows, etc.

1.2. Problem statement

In the development process of a waste heat recovery system based on the organic Rankine cycle a question that arises is how the recovered power will be transmitted to the driveline and further to the wheels. In this project, the topic is to integrate the waste heat recovery system into the complete vehicle model and then to add and compare transmission models to transfer recovered power.

1.3. Assumptions and delimitations

- This report only deals with long haul heavy duty Diesel trucks with its related driving conditions.
- The conventional vehicle model is built on Simulink and works well.
- The waste heat recovery model is built on Simulink but needs to be adapted to the simulation platform in order to be integrated.
- The waste heat recovery model has already shown good results in stationary conditions on specific operating points but has not been tested yet in real driving conditions.
- The simulated model was equipped with a turbine as expander.
- The cooling model calibration will only be done for one engine (VT-NA MD13 500hp US10). Modifications regarding fan parameters, radiator parameters and engine heat losses may be different for other engines.

1.4. Outline

For reasons explained later, a cooling system model has to be created and calibrated. This is done in chapter 2. Then an overview of transmissions types that are suitable for waste heat recovery applications is done in chapter 3. Once the model is completed and ready, simulations are done in chapter 4 and results are shown and compared. Finally, the conclusion of the thesis is drawn in chapter 5.

Chapter 2: Cooling system model

2.1. Need for a cooling system model

One of the main requirements that the waste heat recovery system must fulfill is that it must not affect engine performance. This involves not affecting cooling performance.

As seen in 1.1.2, the condenser rejects heat. The amount of heat can be as high as 85% to 90% of the recovered heat (50kW to 100kW). Heat has to be dissipated in the ambient in some way. The most convenient way is to place the condenser or an intermediate cooling circuit with a radiator in front of the truck where fresh air is entering (i.e. close to the main radiator). Thus one understands that air temperature around the main radiator will be affected, thus reducing heat exchange possibilities in the main radiator and finally cooling performance. In normal driving conditions, i.e. at high vehicle speed and part load, when a lot of fresh air is entering through the nose and with moderate heat rejection from the engine to the coolant and at reasonable ambient temperature, the radiator is oversized and heat rejection limit is very high. On the contrary, when the vehicle speed is low and the engine load is high in up-hills for example or if the ambient temperature is very high, it is crucial to evaluate coolant temperature to determine whether it is possible to reject extra heat coming from the condenser or not in order not to affect engine performance.

One also has to note that extra fan engagement should be strictly avoided since its maximum power (as shown in Figure 14) can exceed recovered power resulting in a negative power output.

The basic layout of a truck cooling system is depicted in Figure 9.

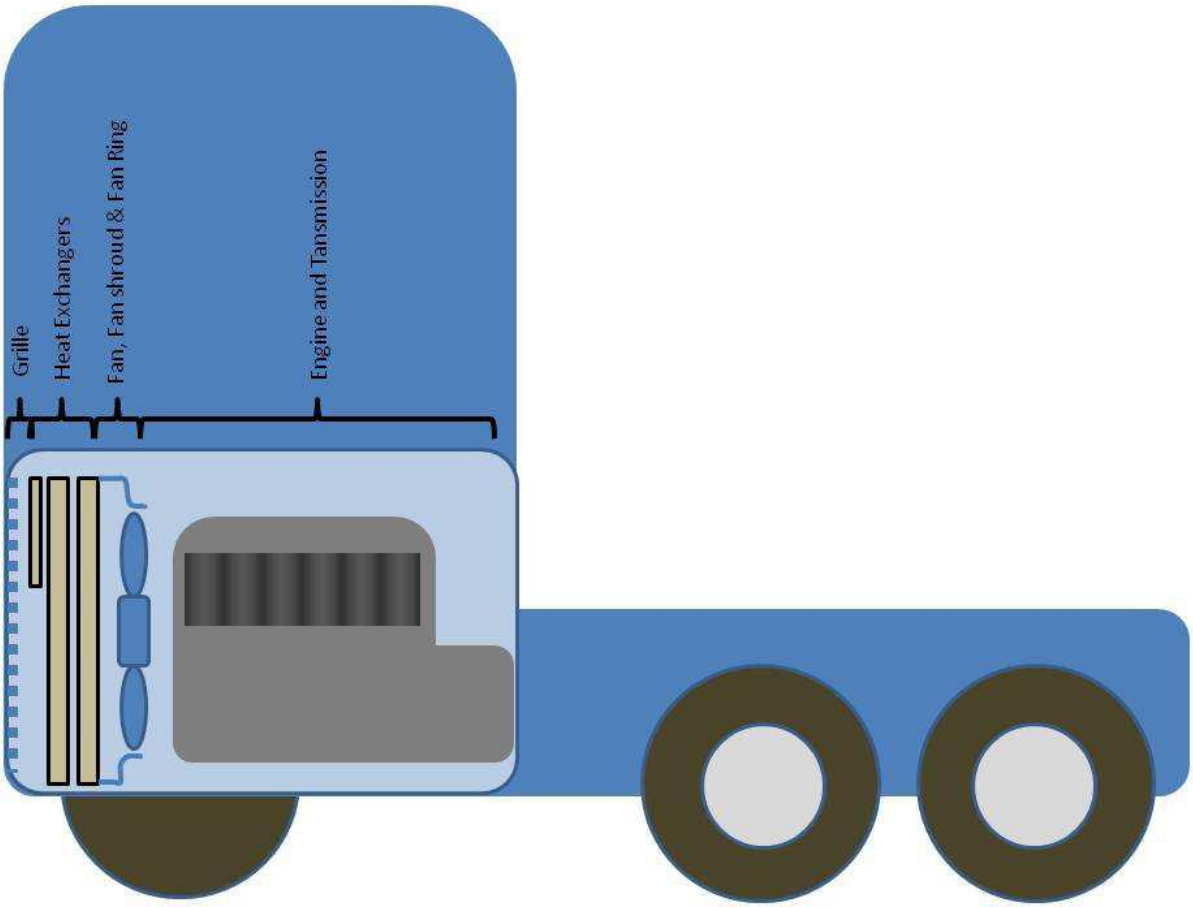

Figure 9: Basic layout of a truck cooling system [5]

2.2. Overview

The aim of the cooling system is to estimate, in a rather simple but accurate way, air, coolant and low temperature coolant temperatures in different nodes of the system as well as fan power consumption.

Computation nodes are:

- Charge air cooler, outlet air
- Low temperature radiator, outlet air
- Low temperature radiator, outlet coolant
- Main radiator, outlet coolant
- Engine, outlet coolant

Three models for three different cooling package configurations have been created. Only one has been used for simulations.

There is no contribution of the EGR cooler to the coolants and air temperatures in the model since EGR gases are supposed to be cooled down thanks to the waste heat recovery system. In other words, EGR cooling is already taken into account in the low temperature radiator block.

As shown in Figure 10, the cooling model is composed of five sub models that interact between each other:

- Engine thermal model
- Charge air cooler model
- Low temperature radiator
- Main radiator
- Air flow model

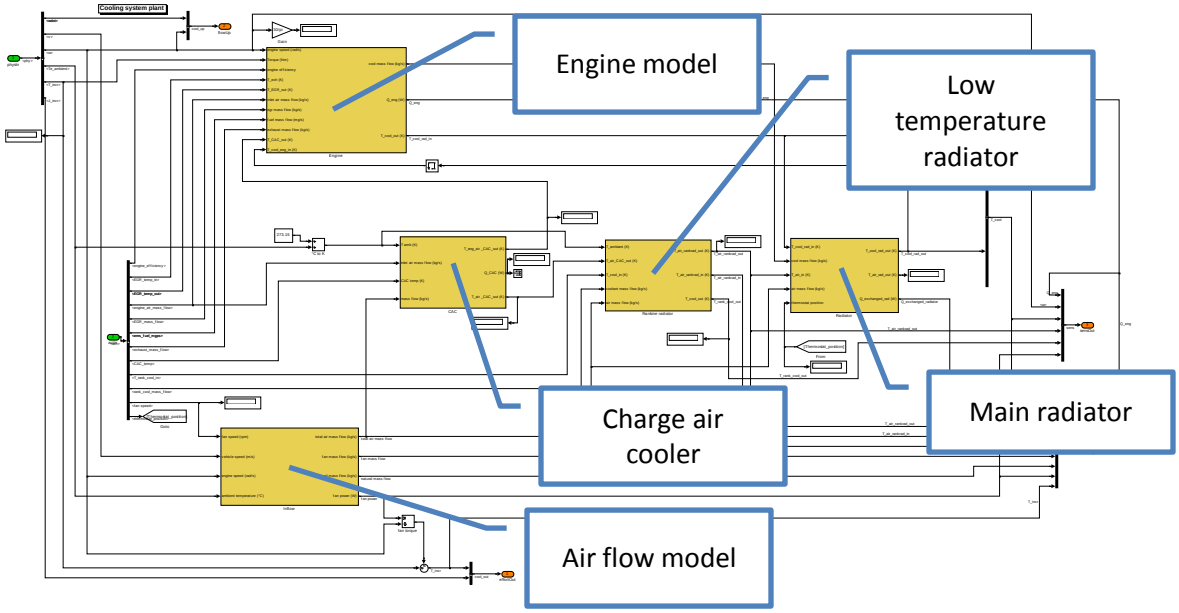

Figure 10: Cooling system model

2.3. Engine thermal model

The engine model takes engine speed, engine torque, engine efficiency, fuel flow, air, exhaust and EGR temperatures and flows as input and outputs coolant temperature increase based on heat rejection from engine to coolant and oil.

There is no distinction made between fuel energy going to the coolant and fuel energy going to the oil since the oil cooler is cooled down by the coolant.

The basic principle used in this component is that energy entering the engine is conserved:

$$\dot{Q}_{coolant} + \dot{Q}_{oil} = \dot{Q}_{fuel} - P_{brake} - \dot{Q}_{exhaust} - \dot{Q}_{miscellaneous} \quad \textbf{2-1}$$

Where

$$P_{brake} = \eta_{engine} * \dot{Q}_{fuel} \quad \textbf{2-2}$$

$$\dot{Q}_{exhaust} = \dot{m}_{exhaust} * c_{p_{exhaust}} \left(\frac{\dot{m}_{charge\ air}}{\dot{m}_{fuel}} \right) * (T_{exhaust} - T_{air}) \quad \textbf{2-3}$$

$\dot{Q}_{miscellaneous}$ has been calibrated so that heat to coolant rejections fit with engine measurements at steady state conditions for different engine loads (or torques) and around 1250 rpm which is the most frequent engine speed at cruising conditions. The model uses the function of engine load displayed in Figure 11.

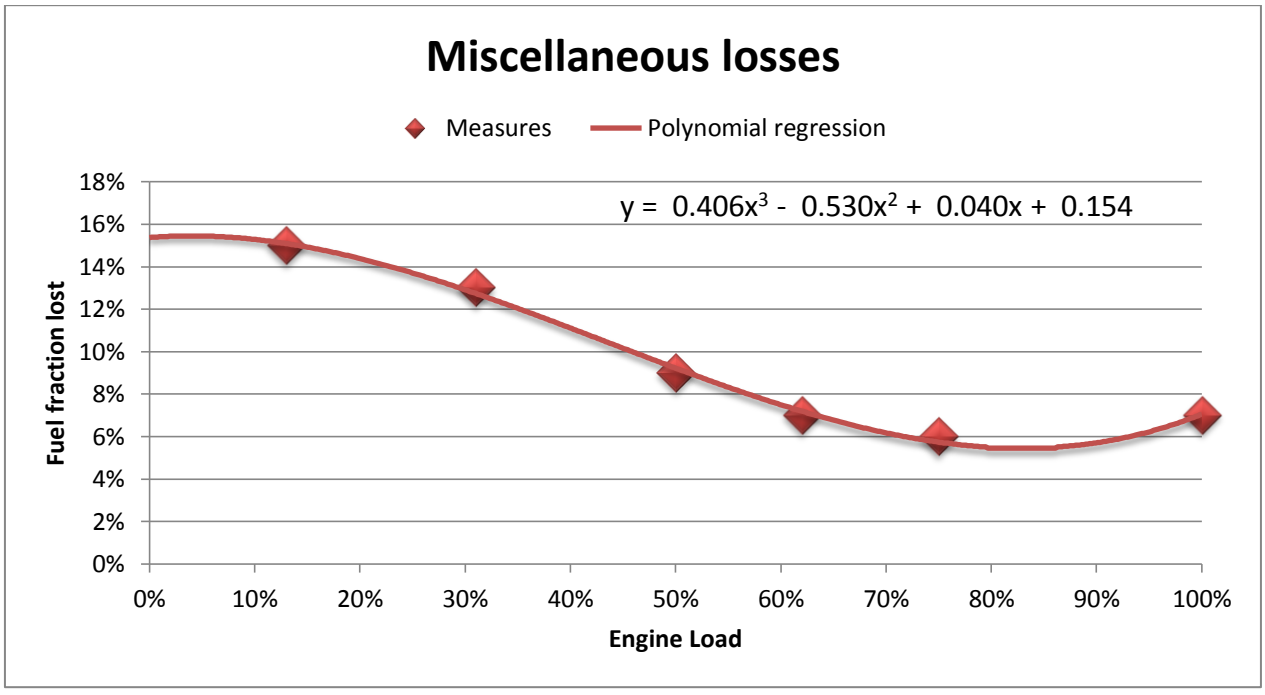

Figure 11: Miscellaneous losses measures and model for a VT-NA MD13 500hp US10 engine

2.4. Fluid-air radiator model

All radiator models take air and fluid inlet temperatures and flows as inputs and output air and fluid outlet temperatures.

Computation is based on the following thermodynamic equations, the fluid at stake being either charge air for the charge air cooler or coolant for the low temperature radiator and the main radiator.

$$\dot{Q} = \dot{m}_{fluid} * c_{p_{fluid}} * \eta * \left| T_{in_{fluid}} - T_{in_{air}} \right| \quad \textbf{2-4}$$

$$T_{out_{air}} = T_{in_{air}} + \frac{|\dot{Q}|}{\dot{m}_{air} * c_{p_{air}}} \quad \textbf{2-5}$$

$$T_{out_{fluid}} = T_{in_{fluid}} - \frac{|\dot{Q}|}{\dot{m}_{fluid} * c_{p_{fluid}}} \quad \textbf{2-6}$$

For the charge air cooler, a constant effectiveness of 95% is assumed whereas an effectiveness table (see Figure 12) as function of air and fluid mass flows is used for the two radiators.

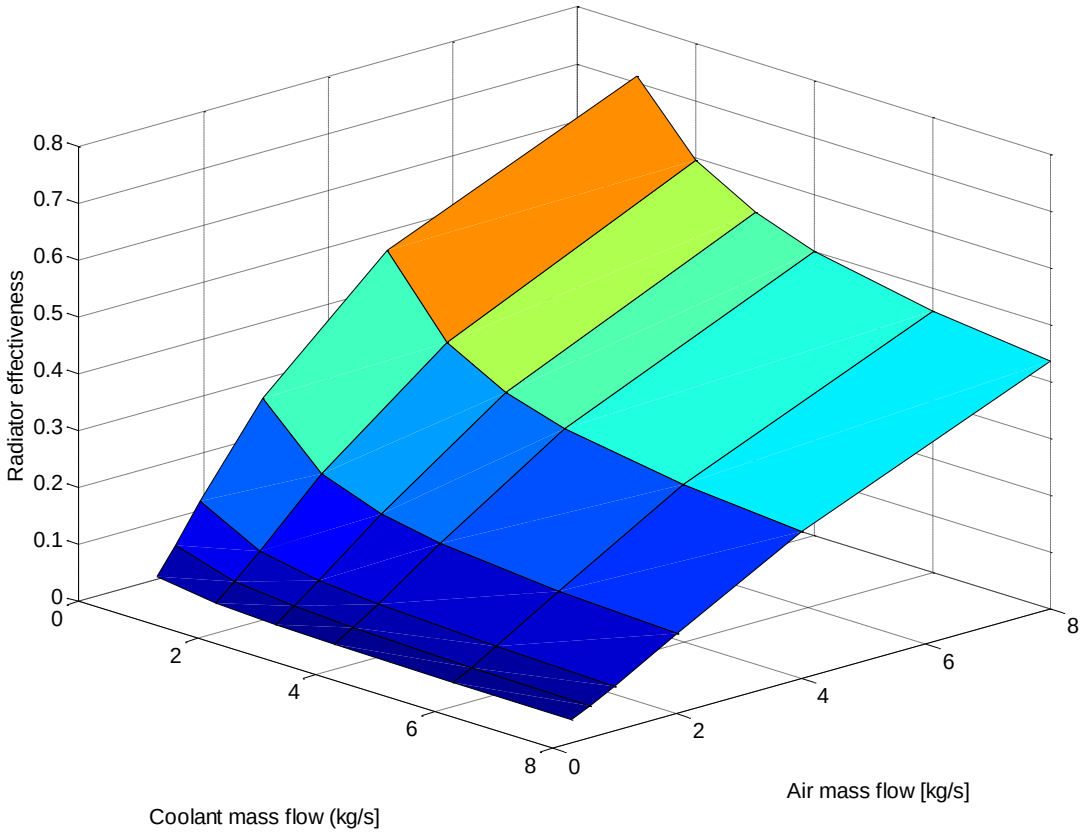

Figure 12: Radiator effectiveness

2.5. Thermostat model

The thermostat aims to regulate coolant temperature, opening or closing a valve to respectively direct or bypass the fluid to the main radiator depending on the coolant temperature. Its dynamic behavior is modeled as a first order transfer function with a faster dynamic response while opening ($\tau = 20\ s$) and a slower response while closing ($\tau = 100\ s$).

Thermostat opening and closing curves as function of coolant temperature are depicted in Figure 13.

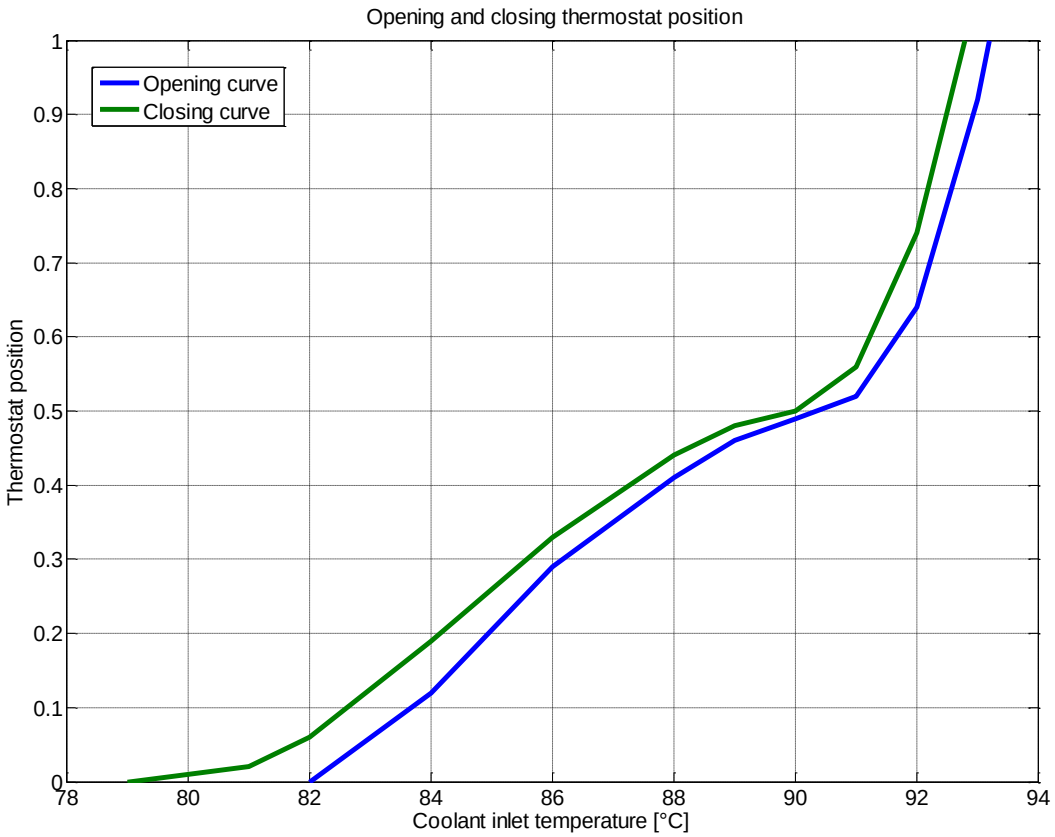

Figure 13: Opening and closing thermostat position

2.6. Air flow model

The air flow is computed from vehicle speed, fan speed and engine speed and outputs air flow and fan power consumption. The total entering air flow is the sum of natural air flow and forced air flow.

$$\dot{m}_{air} = \dot{m}_{natural} + \dot{m}_{forced} \quad \textbf{2-7}$$

2.6.1. Natural air flow model

The natural flow represents the amount of air that naturally enters the truck nose thanks to the vehicle movement. Due to the nose geometry and aerodynamic behavior, the velocity of air entering the nose is about one tenth of the upstream air velocity.

$$\dot{m}_{natural} = 0.1 * v_{vehicle} * A_{rad} * \rho_{air} \quad \textbf{2-8}$$

$v_{vehicle}$ is the vehicle speed, A_{rad} the radiator front area and ρ_{air} the air density.

2.6.2. Forced air flow model

The forced air flow represents the amount of air that is sucked up from the ambient to the nose via the fan.

$$\dot{m}_{forced} = C_{flow} * n_{fan} * \rho_{air} \quad \textbf{2-9}$$

C_{flow} is a constant that depends on fan characteristics, n_{fan} is the fan rotational speed and ρ_{air} the air density.

The forced flow is generated by the fan that uses power from the engine to convert it into air motion. The power consumption is given by:

$$P_{fan} = C_{fan} * \rho_{air} * n_{eng} * r * {n_{fan}}^2 \quad \textbf{2-10}$$

C_{fan} is a fan characteristics dependent constant, ρ_{air} the air density, n_{eng} the engine rotational speed, r the fan speed ratio and n_{fan} the fan rotational speed.

The fan is coupled to the crank shaft via a viscous coupling. Thus the fan speed can be controlled to match a demand. The real demand is complex and depends on many parameters from different components. To keep the model rather simple, only the coolant temperature will be taken into account to compute the fan speed demand. This model part is often referred as outer control loop. Fan speed demand is first determined using a table, then there is also an integral gain tied to the temperature difference between current and set temperatures (99°C) of 1.5 rpm/°C.s. Due to the engine coupling, the fan speed is also limited according to the following equation:

$$n_{fan} \leq n_{eng} * r * \left(1 - slip_{fan}\right) \quad \textbf{2-11}$$

$$slip_{fan} \approx 5\% \quad \textbf{2-12}$$

Finally, Figure 14 shows fan performance when it is fully engaged, i.e. when:

$$n_{fan} = n_{eng} * r * \left(1 - slip_{fan}\right) \quad \textbf{2-13}$$

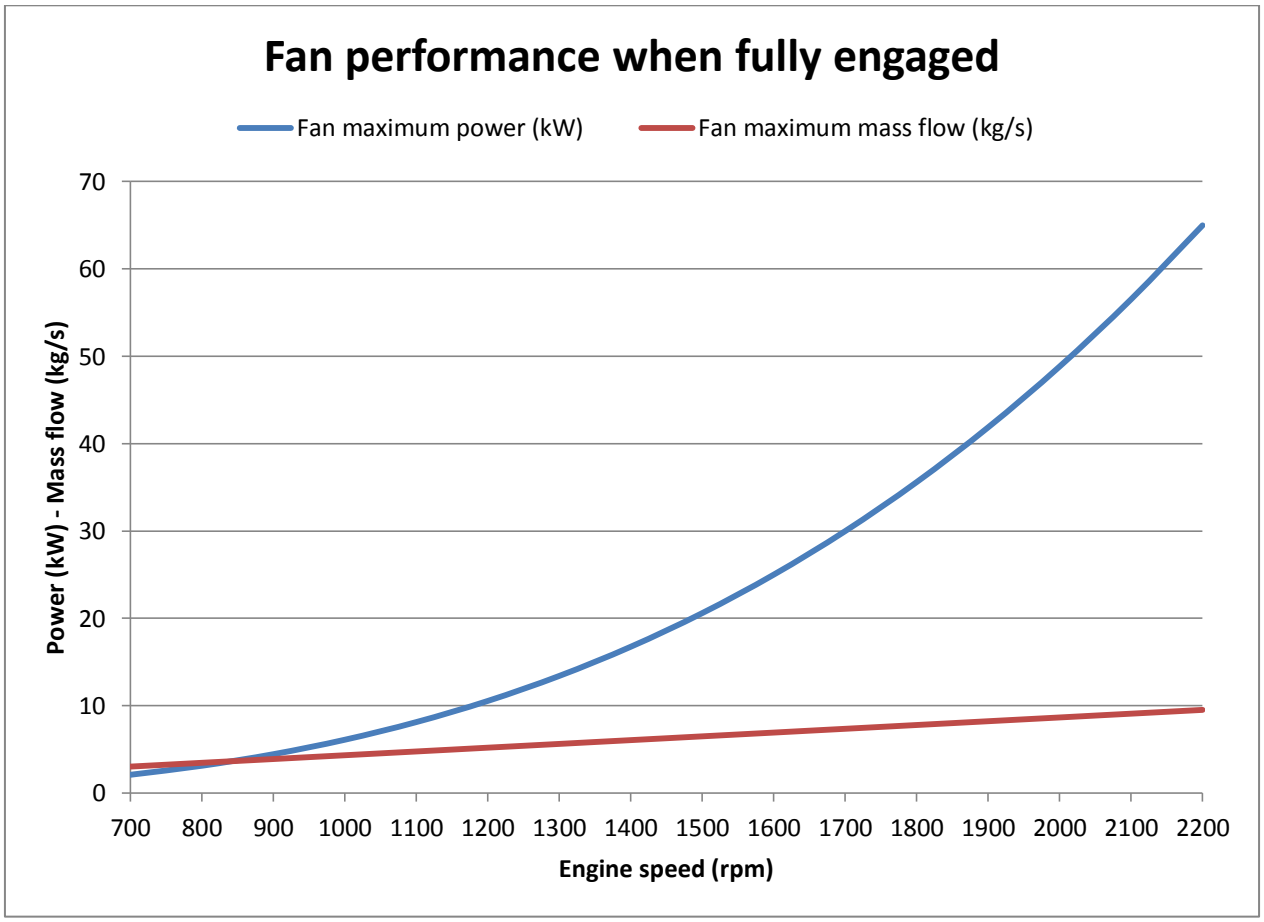

Figure 14: Fan performance for a fully engaged fan

2.7. Model validation

Once the cooling model has been built, validation tests were done and results are shown in Figure 15, Figure 16 and Figure 17.

Tests were done in stationary conditions at constant engine speed (1285 rpm) and for different operating points that correspond to different engine percent loads. Ambient temperature was set to 25°C.

Results are compared to engine test rig measures in stationary conditions.

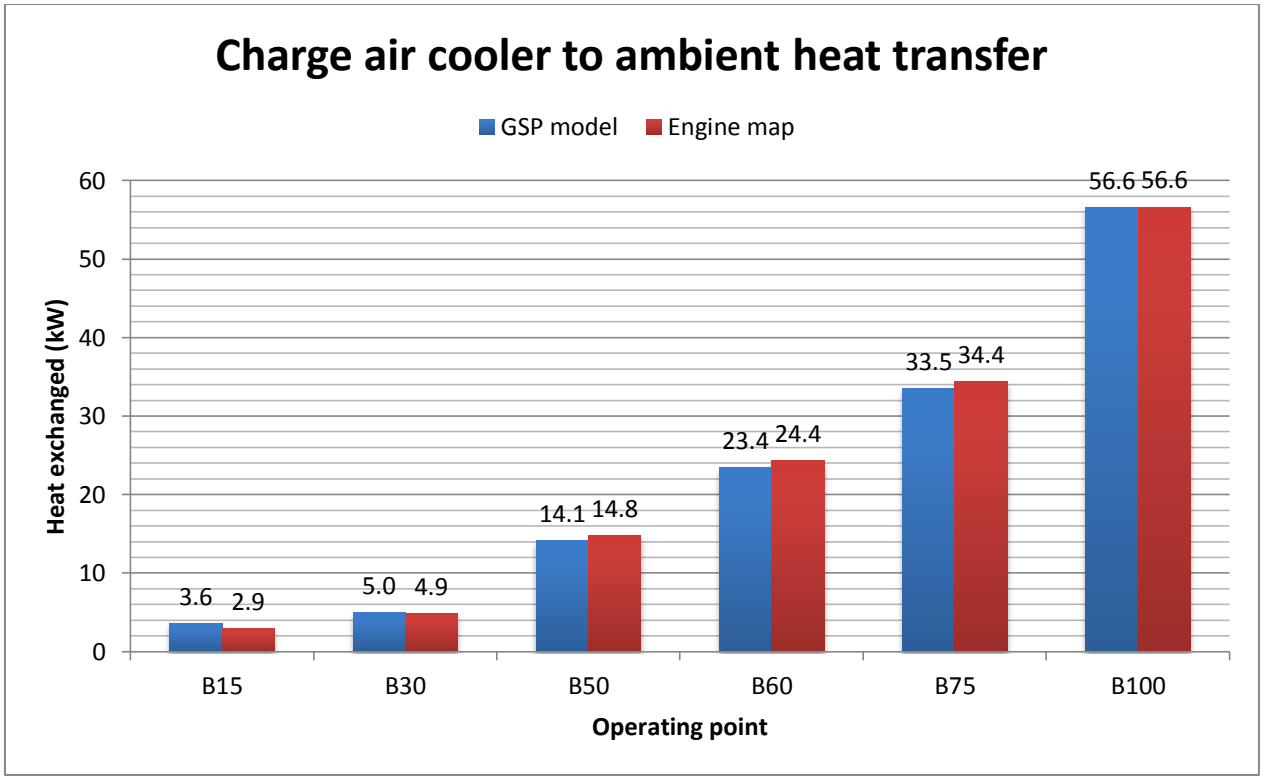

Figure 15: Charge air cooler to ambient heat transfer

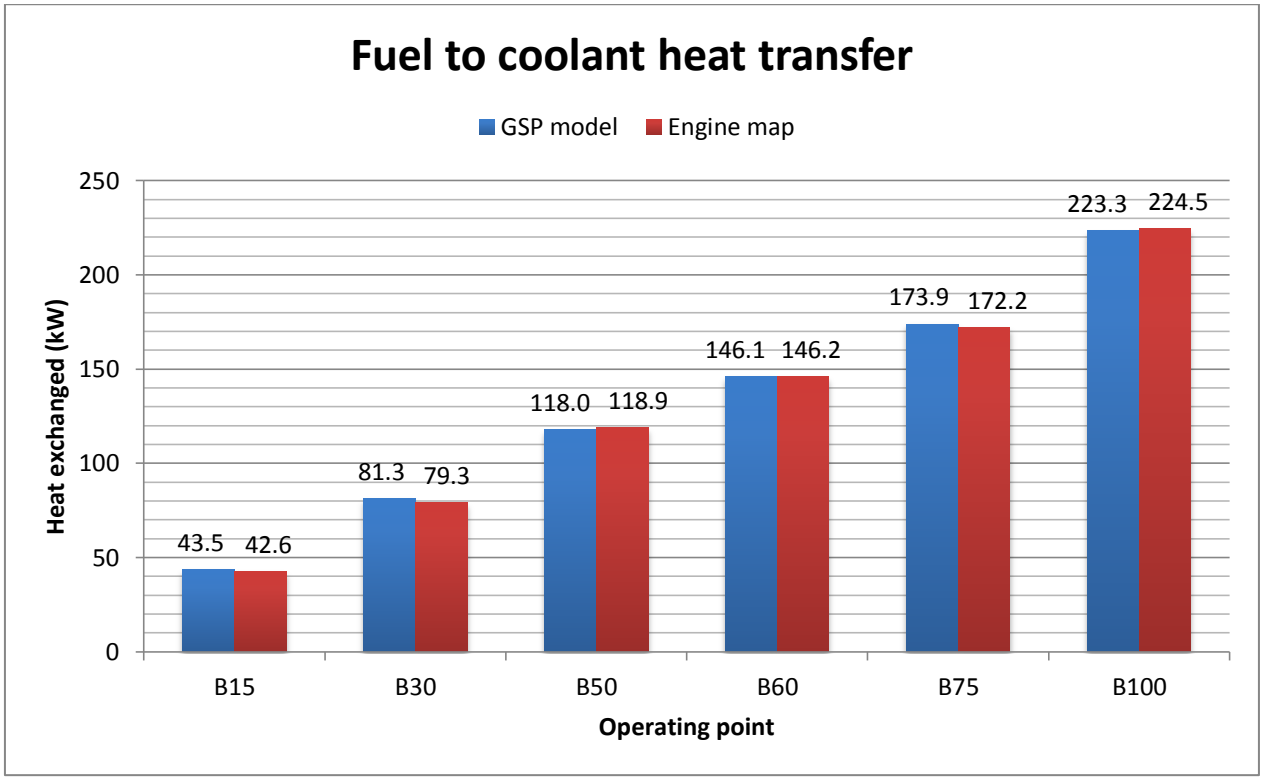

Figure 16: Fuel to coolant heat transfer

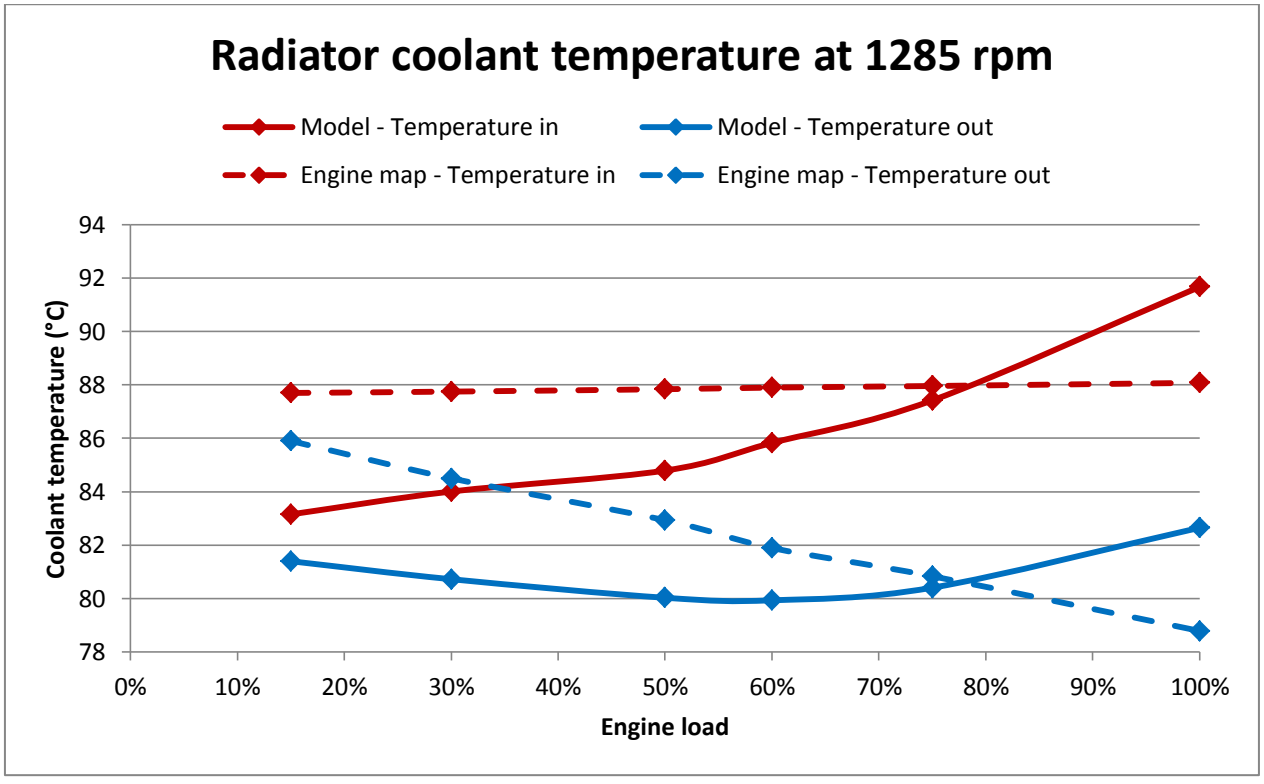

Figure 17: Radiator coolant temperatures at 1285 rpm

One the one hand, Figure 15 and Figure 16 show very good fittings between model predictions and measures. It means that the charge air cooler and the engine model are well modeled and calibrated.

One the other hand, Figure 17 shows some discrepancies between predictions and measures especially for low engine loads even if differences remain lower than 5°C. However, temperature differences between inlet and outlet ports are equal when comparing simulation results to engine measures. Discrepancies can have multiple causes either inherent to the model or to the measurement itself:

- Lack of accuracy in the radiator effectiveness. For example, it is not external temperature dependent.
- Lack of accuracy in the thermostat opening and closing curves.
- The temperature control in the engine test rig is different than the regular temperature control since it is water-cooled; the radiator inlet temperature is kept at a target temperature of 88°C. Thus those strategy differences result in different temperature levels.

Chapter 3: Transmission overview

3.1. System requirements

The complete waste heat recovery transmission system must comply with the following requirements:

- Input speed can be as high as 150000 rpm with extreme values up to 200000 rpm in case a turbine is used as expander.
- Input power can be up to 15 kW.
- If the expander is a piston machine with high friction losses, the transmission must allow uncoupling the expander and the output shaft to avoid dissipating energy through friction.
- In case of large speed ratios, high amplitude speed variations must be damped in order not to destroy the expander because of output speed variations that are multiplied through the large speed ratio. This is no longer a problem when variable speed ratios are possible due to speed adjustments.

3.2. Comparison methodology

The goal of the comparison is to find the best suitable configuration for a given expander type and expander output shaft speed. The best configuration will be a trade off between several transmission characteristics.

3.2.1. Input speed range

Input speed range is an important factor to consider since it will determine whether a possible transmission configuration can be used as a stand-alone system or must be coupled with another speed reduction system. Thus increasing the system complexity and reducing the overall efficiency.

3.2.2. Speed ratio range

Speed ratio also called reduction ratio is defined as the ratio between input and output speeds ($r_{speed} = \frac{\omega_{in}}{\omega_{out}}$). This ratio gives the ability of the transmission to reduce speeds between input and output shafts and determines if extra reduction is needed.

3.2.3. Transmission efficiency

Efficiency is likely to be the most important point to consider. It is defined as the ratio between output and input power ($\eta = \frac{P_{out}}{P_{in}} = \frac{T_{out}*\omega_{out}}{T_{in}*\omega_{in}}$). This quantify how much power from the input shaft is transferred to the output shaft and how energy is lost in friction or heat.

3.2.4. Weight and size

Weight and size are two parameters that have to be taken into account for packaging purpose. The smaller and lighter components are, the easier it will be to be integrated in a truck.

3.2.5. Price

Price obviously has to be taken into account in the final decision process to ensure a reasonable overall price for the waste heat recovery system. However prices will not be compared in this comparison study. Price can be first assumed to be proportional to the system complexity.

3.3. Global transmission types

Three different transmission types can be defined depending on the kind of energy that is transmitted through components.

3.3.1. Mechanical transmissions

A purely mechanical transmission only involves mechanical component such as gears, pulleys and belt or more refined mechanical components. Energy remains mechanical all along the transmission process.

The following mechanical components are compared:

- Simple gear train
- Planetary gear train
- Friction type CVT

3.3.2. Electrical transmissions

A purely electrical transmission involves energy conversion from mechanical energy to electrical energy and then back to mechanical energy. This process involves using generators and motors as well as electronic converters. Storage components such as batteries or super-capacitor can be added to the system to add the possibility to store energy for further use as boost power for instance.

The following electrical components are compared:

- Electrical CVT
- Battery storage
- Super-capacitor storage

3.3.3. Electro-mechanical transmissions

A third transmission type can be defined. This type is a combination of a purely mechanical and a purely electrical transmission. Input power will be split into two branches. The first is a purely mechanical branch whereas the second is a purely electrical branch. Split powers are finally merged together on the output shaft.

3.4. Mechanical transmissions

3.4.1. Simple gear trains

3.4.1.1. Main characteristics

Table 1 shows simple gear trains main characteristics.

Table 1: Simple gear train characteristics

Input speed range	Very high
Speed ratio range	Up to 7 per stage For n stages in series configuration, speed ratio up to 7^n
Transmission efficiency	From 98% to 99% per stage For a single stage train, the lower ratio, the higher efficiency For n stages in series configuration with η % efficiency, transmission efficiency up to η^n %
Weight	About 1kg
Size	About a dozen centimeters as gear diameter

The number of stage n required is chosen according to the following formula:

$$\begin{cases} i^{n-1} \leq r_{speed} \leq i^n \\ i : \text{single stage ratio} \\ r_{speed} : \text{desired ratio} \end{cases} \quad \textbf{3-1}$$

Thus, the maximum efficiency is obtained when n is minimized, and after that, when i is minimized.

A 2 stages gear train in series configuration is depicted in Figure 18.

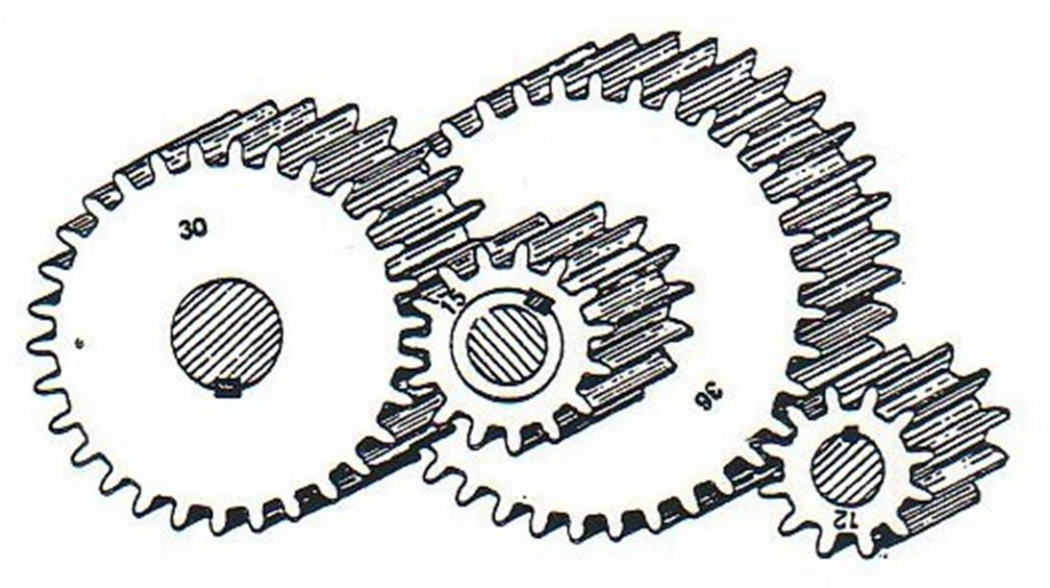

Figure 18: 2-stages gear train

3.4.1.2. Advantages

The main advantage of this component is its very high efficiency, even with two or three stages, compared to more complex components. There is no need for any other system since input speed can be very high and high reduction ratios can be performed if several stages are used in series configuration. The system is also rather simple and compact.

3.4.1.3. Drawbacks

The main drawback is the fixed gear ratio. Expander will thus not always operate at its maximum efficiency. This alternative is a permanent fixed ratio coupling that thus requires being uncoupled thanks to a clutch or viscous coupling to comply with uncoupling and damping requirements.

3.4.2. Planetary gear trains

3.4.2.1. Main characteristics

Table 2 shows simple gear trains main characteristics.

Table 2: Planetary gear train characteristics

Input speed range	Very high
Speed ratio range	Up to 10 per stage For n stages in series configuration, speed ratio up to 10^n
Transmission efficiency	About 98% per stage For n stages in series configuration with η % efficiency, transmission efficiency up to η^n %
Weight	About 1kg
Size	About a dozen centimeters as diameter, depth is a few centimeters per stage

The number of stage n required is chosen according to the following formula:

$$\begin{cases} i^{n-1} \leq r_{speed} \leq i^n \\ i : \text{single stage ratio} \\ r_{speed} : \text{desired ratio} \end{cases} \quad \textbf{3-2}$$

Thus, the maximum efficiency is obtained when n is minimized, and after that, when i is minimized.

Figure 19 shows a single stage planetary gear train.

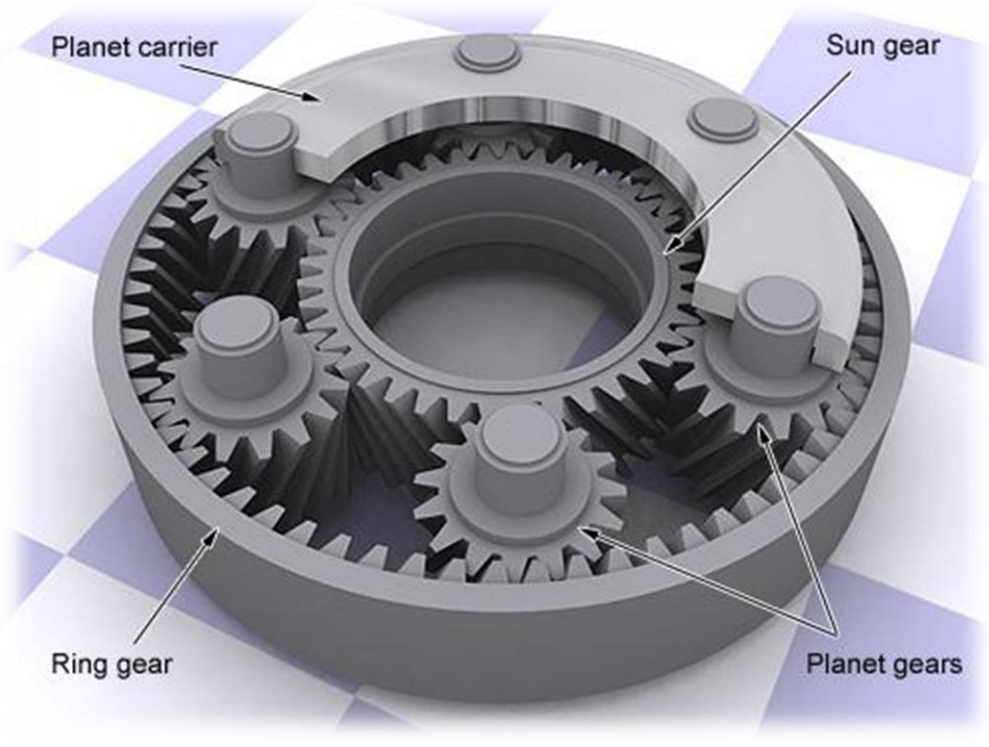

Figure 19: Planetary gear train [6]

3.4.2.2. Advantages

Advantages of this system are almost the same as for the simple gear train except that higher ratios can be reached with the same number of stage. This makes the system even more efficient.

3.4.2.3. Drawbacks

This system also operates with a fixed gear ratio as for the simple gear train. Moreover the system and especially multiple stages planetary gear train is more complex. This system also suffers from the lack of uncoupling and damping abilities.

3.4.3. Friction type CVT

3.4.3.1. Main characteristics

There are different kinds of friction type CVT based on different designs, some examples are shown in Figure 20 and Figure 21. Motion and power are always transferred thanks to friction between moving parts. The most known technologies are:

- Belt or chain CVT: it basically consists of two pulleys, one driving and one driven pulley, and a belt or chain linking them all together. Most of the time, each pulley is composed of a fixed and moveable pulley sheaves that are located on opposite sides of the pulleys. Combined pulley sheaves displacements vary pulley radii and thus the speed ratio defined as $r_{speed} = \frac{\omega_{out}}{\omega_{in}} = \frac{R_{in}}{R_{out}}$.

Friction between pulleys and belt and hydraulic forces, often referred as clamping forces, that move pulley sheaves and push the belt against the pulleys are the main causes of power loss.

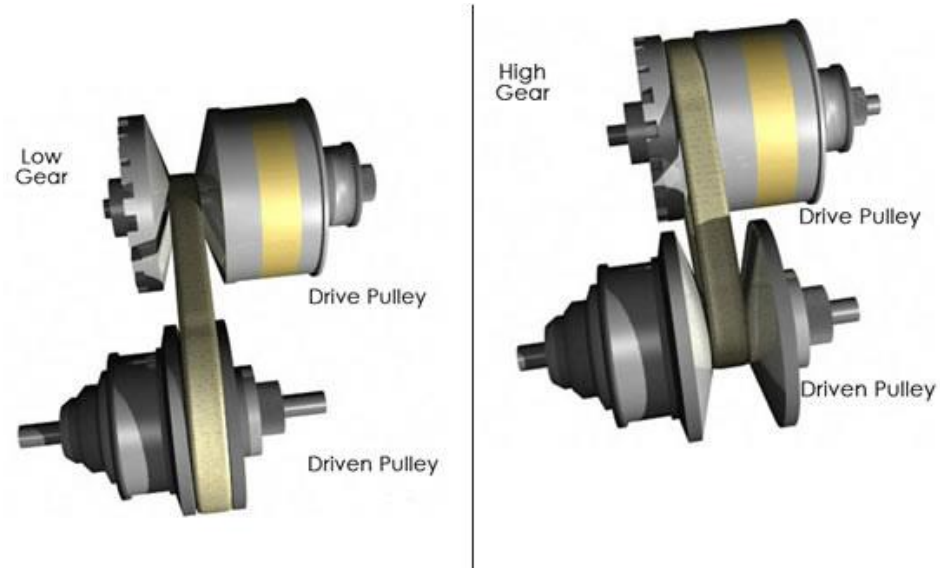

Figure 20: Belt CVT [7]

- Toroidal CVT: this concept consists of two half or full toroidal discs with two power rollers in between. The contact between discs and power rollers is kept by mean of a loading force generated by a loading cam or a hydraulic piston. This consumes part of the energy transferred. The tilting rotation angle of the power rollers defines the speed ratio $r_{speed} = \frac{\omega_{out}}{\omega_{in}} = \frac{R_{in}}{R_{out}}$.

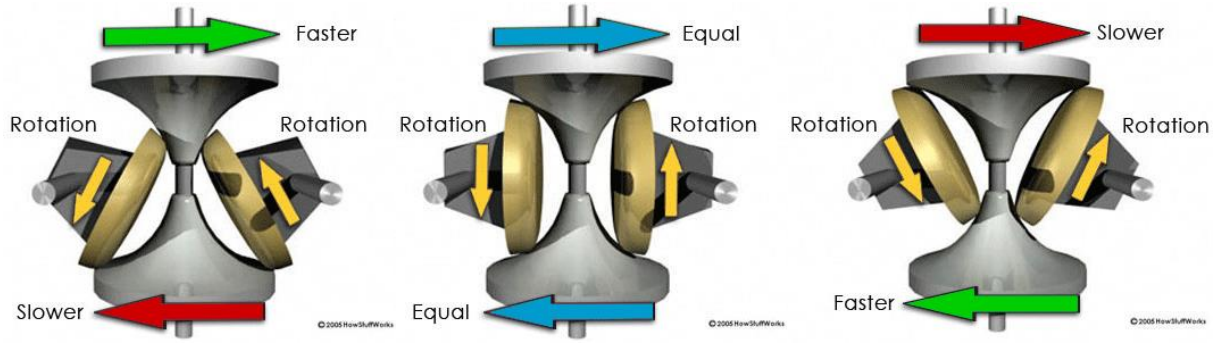

Figure 21: Half toroidal CVT [7]

Main CVT charateristics are presented in Table 3.

Table 3: Friction type CVT characteristics

Input speed range	Up to 12000 rpm
Speed ratio range	Up to 6
Transmission efficiency	▪ Chain/belt CVT: Up to 85-90% ▪ Toroidal CVT: Up to 85-90%
Weight	About 1 kg (rough estimation, proportional to bigger CVT currently used)
Size	▪ Chain/belt CVT: Approximately 15 x 10 cm (rough estimation, proportional to bigger CVT currently used) ▪ Toroidal CVT: No data found

3.4.3.2. Advantages

The most important advantage of this technical solution is the possibility to vary the speed ratio so that the expander always operates at its maximum efficiency. Rubber belt CVTs are quite soft and can damp speed variations to the expander shaft.

3.4.3.3. Drawbacks

Downsides of this component are numerous. Speed and speed ratio ranges are limited, thus requiring the addition of an extra reducer for the CVT system to operate within normal working conditions. This system cannot be uncoupled and thus require adding an extra coupling device.

3.5. Electrical transmission

3.5.1. Direct electrical transmission – Electrical CVT

3.5.1.1. Main characteristics

It is possible to build a fully electric system that offer the possibility to vary the speed ratio. This complex system uses several components to successively convert mechanical power to alternative current thanks to a synchronous AC generator then adapt current frequency to optimize the speed ratio thanks to a combination of electronic converters and finally convert alternative current back to mechanical energy thanks to a synchronous AC motor.

A frequency adapter is usually composed of inverter type converters that first convert alternative current to continuous current, output current is then smoothed with a capacitive filter, and finally continuous current is converted back to alternative current with controlled frequency.

The typical efficiency of electronic converters is around 95% and the typical efficiency of synchronous AC motors or generators is comprised between 91% and 98%.

New generations of permanent magnet high speed generators and motors have shown increases in input speeds resulting in values up to 100000 rpm according to some manufacturers such as e+a[1] or Calnetix[2], this enabling direct coupling between turbo machineries and generators.

The maximum speed ratio depends both on the current frequency ratio between the generator and the motor and on numbers of pole pairs of the electric machines. In synchronous machines the rotational speed Ω is linked to the current frequency ω with the following formula: $\Omega = \frac{\omega}{p}$ where p is the number of pole pairs. Thus, choosing one pair of poles for the generator and 3 or 4 pairs for the motor increases the speed ratio range.

Main electric CVT characteristics are shown in Table 4.

Table 4: Electric CVT characteristics

Input speed range	Up to 200000
Speed ratio range	Very high
Transmission efficiency	$\eta \approx 95\ \%^4 = 81\%$
Weight	About 1 kg per motor/generator
Size	About 10 x 10 cm per motor/generator

Figure 22 and Figure 23 shows some details about the system layout.

[1] http://www.highspeedgenerator.com
[2] http://www.calnetix.com

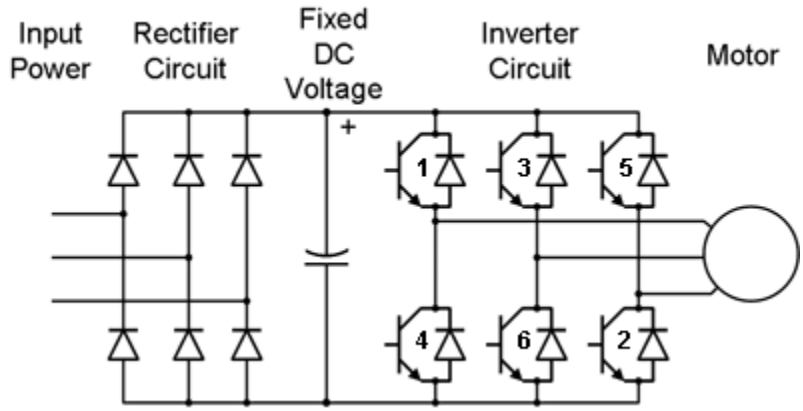

Figure 22: Three phases variable frequency inverter [8]

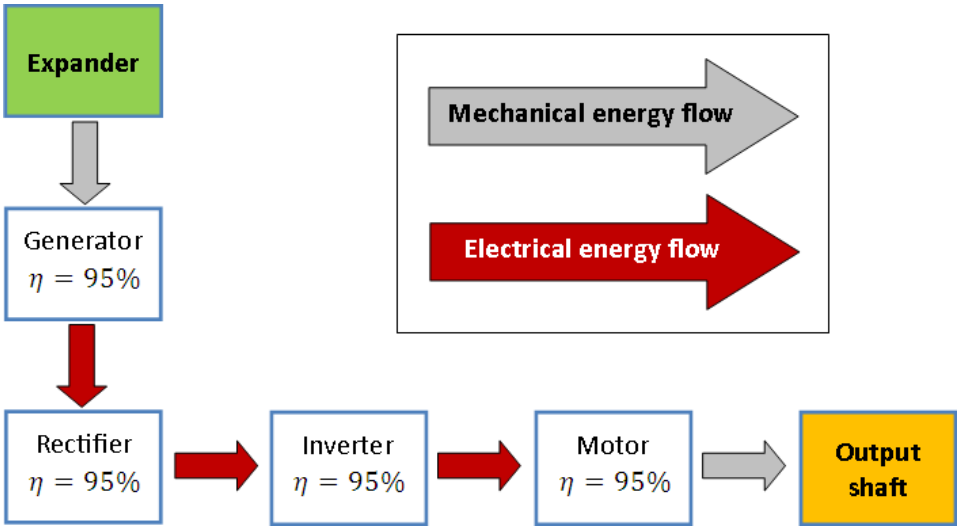

Figure 23: Electrical transmission principle

3.5.1.2. Advantages

Main advantages of this coupling solution are high upper limit in input speed as well as the possibility to control the speed ratio to adapt to expander best operating conditions. This system also shows very good modularity performance since there is no mechanical transmission between expander output shaft and engine or wheel shaft. Thus the waste heat recovery system and the engine are completely independent and can be set anywhere in the truck. Besides it offers the possibility to uncouple input and output shafts when needed provided resistors are mounted to dissipate produced energy.

3.5.1.3. Drawbacks

As drawbacks, the system is quite complex and suffers from a rather low efficiency compared to other alternatives already explained.

3.5.2. Micro-hybrid system with battery storage

3.5.2.1. Main characteristics

The previous system can be further improved adding a battery between the rectifier and the inverter as seen in Figure 24. It enables to store the recovered energy for later use when extra power is needed such as during hill climbing or acceleration to avoid the engine to run in transient conditions.

Table 5 shows compared performances of typical battery types used in automotive applications. It clearly appears that Lithium-ion and Lithium-ion Polymer batteries are the more suitable for waste heat recovery applications. Main choosing criteria are first charge/discharge efficiency in order not to waste recovered energy and then specific energy and power to ensure a lightweight solution.

Table 5: Battery types comparison

Battery type	Specific energy (Wh/kg)	Specific power (W/kg)	Charge/discharge efficiency[3]	Cycle durability (cycles)
Lead-Acid	30-40	180	50-92%	500-800
NiMH	30-80	250-1000	66%	1500
Molten-Salt	100	150	No data found	1000
Li-ion	90-160	1800	97-99%	1200
Li-Po	130-200	2800	97-99%	1000

For the battery dimensioning, a maximum power recovery capacity of 10 kW is assumed for the battery. Assuming a maximum recovery time span of 10 minutes (15 km at 90 km/h), with an average power of 8 kW, leads to an energy capacity of 1.4 kWh. This time span seems to be a good trade off between weight saving and storage capacity. Most of the energy will be recovered when driving on flat roads at full speed and extra power will be mainly needed when hill climbing or accelerating, it can then be assumed an increase in power demand lies every 15 km on highways.

Table 6 shows micro-hybrid system main characteristics.

Table 6: Micro hybrid system characteristics

Input speed range	See Direct electrical transmission – Electrical CVT
Speed ratio range	See Direct electrical transmission – Electrical CVT
Transmission efficiency	$\eta \approx 95\%^2 * 98\% * 95\%^2 = 80\%$
Weight	Extra weight due to the battery: ▪ Li-ion: 8.5 kg ▪ Li-Po: 6.5 kg
Size	2 dm^3 for a Li-ion battery

[33] Charge/discharge efficiency takes into account both charge and discharge efficiency.

According to the assumptions made, the most restrictive criterion for battery weight is the energy storage capacity.

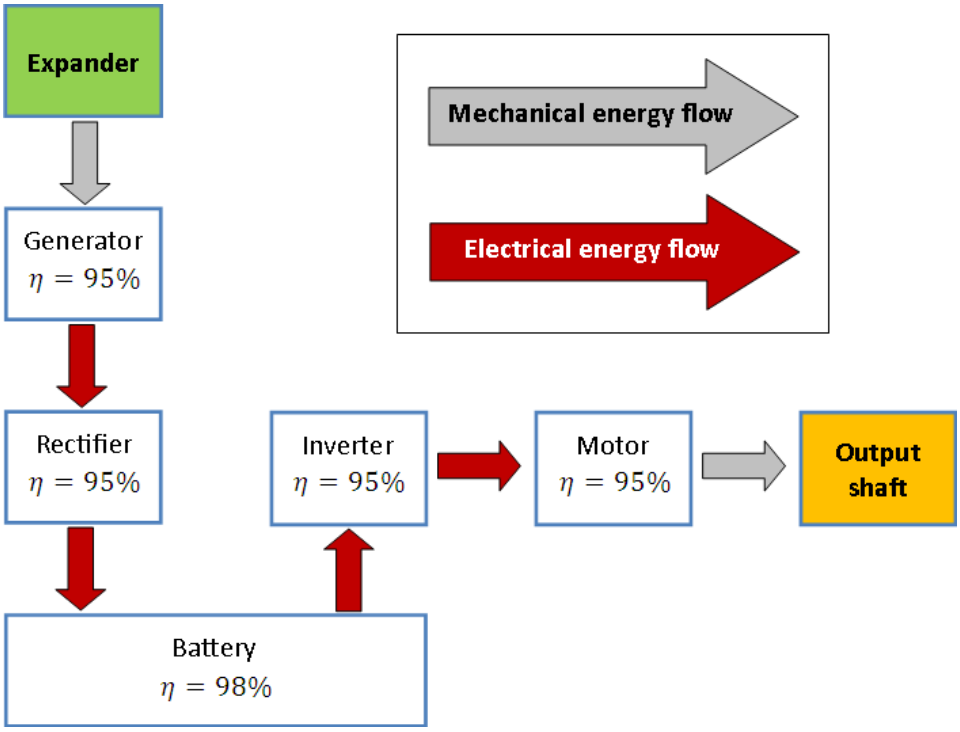

Figure 24: Electrical transmission with battery storage principle

3.5.2.2. Advantages

This system combines advantages of the fully electrical direct transmission and the possibility to store recovered energy for later use when extra power is needed for instance.

3.5.2.3. Drawbacks

The main drawbacks of this alternative are its complexity and heaviness.

3.5.3. Micro-hybrid system with super-capacitor storage

3.5.3.1. Main characteristics

An alternative to the previous system could be to replace the battery with super-capacitors that have much higher power capacities but reduced energy capacity, as seen in Table 7. The Ragone chart in Figure 25 shows specific power and energy of various batteries and capacitors types.

Table 7: Storage types comparison

Storage type	Specific energy (Wh/kg)	Specific power (W/kg)	Charge/discharge efficiency	Cycle durability (cycles)
Super-capacitor	0.1-9	3000-10000	95%	10^5 to 10^6
Li-ion capacitor	10-15	3000-14000	90%	10^4 to 10^5
Li-ion Battery	90-160	1800	97-99%	1200
Li-Po Battery	130-200	2800	97-99%	1000

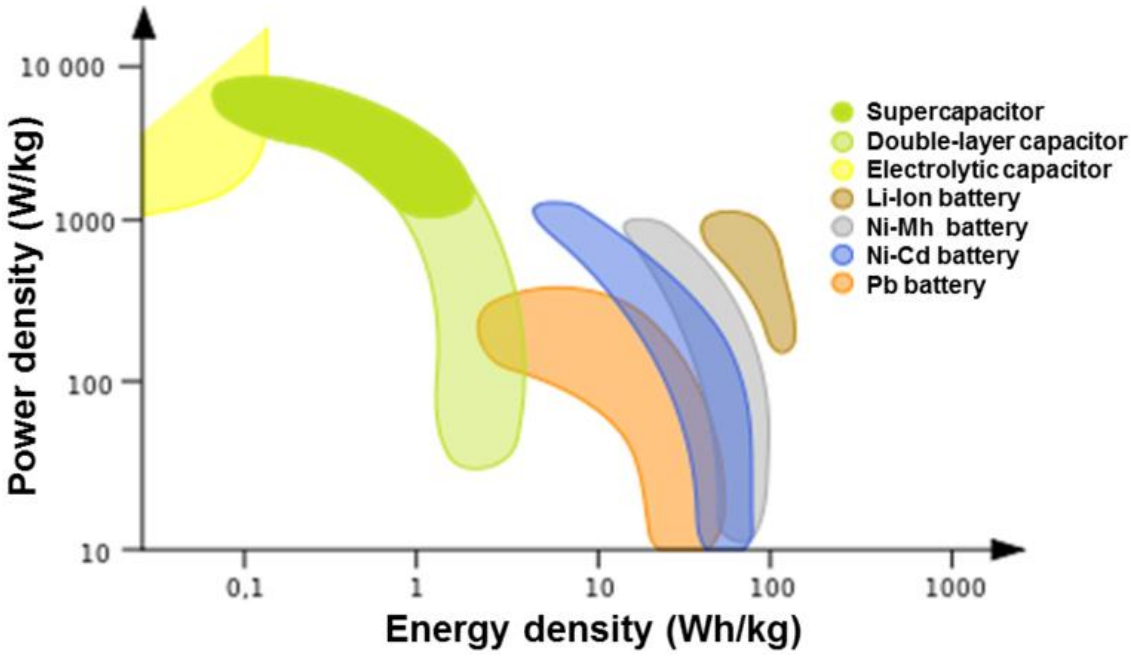

Figure 25: Ragone chart showing power density vs. energy density of various capacitors and batteries [9]

With the assumptions previously made for power recovery capacity and energy autonomy, since the specific energy was already the weakest point, there is no possible improvement replacing the battery with super-capacitors since they have lower specific energies and besides lower efficiencies.

Figure 26 shows how much battery or capacitor weight is needed for given autonomies for different kinds of storage systems.

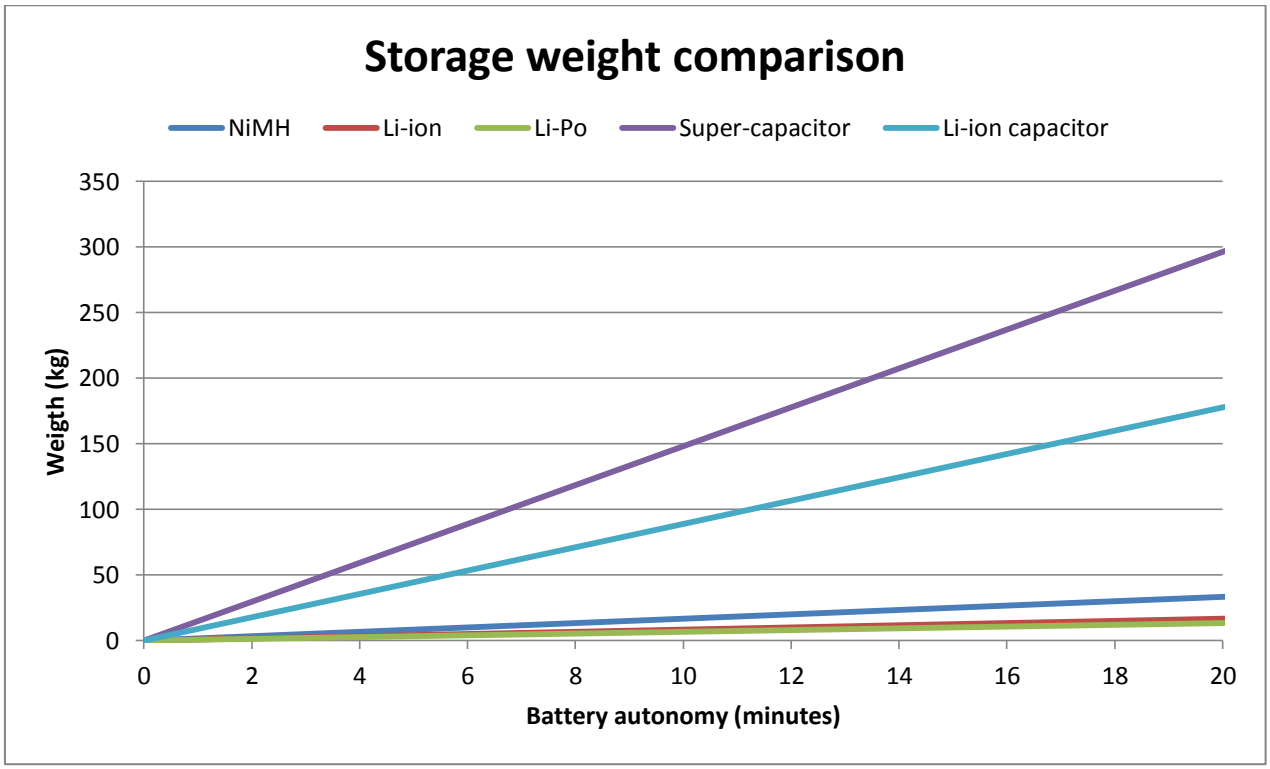

Figure 26: Required storage system weight comparison

3.5.3.2. Advantages

The main advantage is a higher specific power. It also allows more charge/discharge cycles.

3.5.3.3. Drawbacks

The main drawback is a much lower specific energy compared to a Lithium battery. The charge/discharge efficiency is lower as well.

3.6. Electro-mechanical transmission

3.6.1. Power split input configuration

3.6.1.1. Main characteristics

The basic principle of the power split transmission is to split input power such as expander power into two parts. The first part is transmitted through a mechanical path such as gear trains and the second part is transmitted through an electrical path such as the one described in 3.5.1. The aim of such a system is to combine both advantages from the mechanical branch (i.e. a very high efficiency) and from the electrical branch (i.e. the variable gear ratio).

Many power split transmission types exist. The input power split configuration, as described in Figure 27, is commonly used in hybrid vehicles. It is the simplest power split configuration. Some more complex configurations also exist, such as compound power split or two modes power split, and are composed of multiple planetary gears and even clutches and brakes for the most complex ones. Those configurations will not be described here since they are much more complex and bigger and require more development and control.

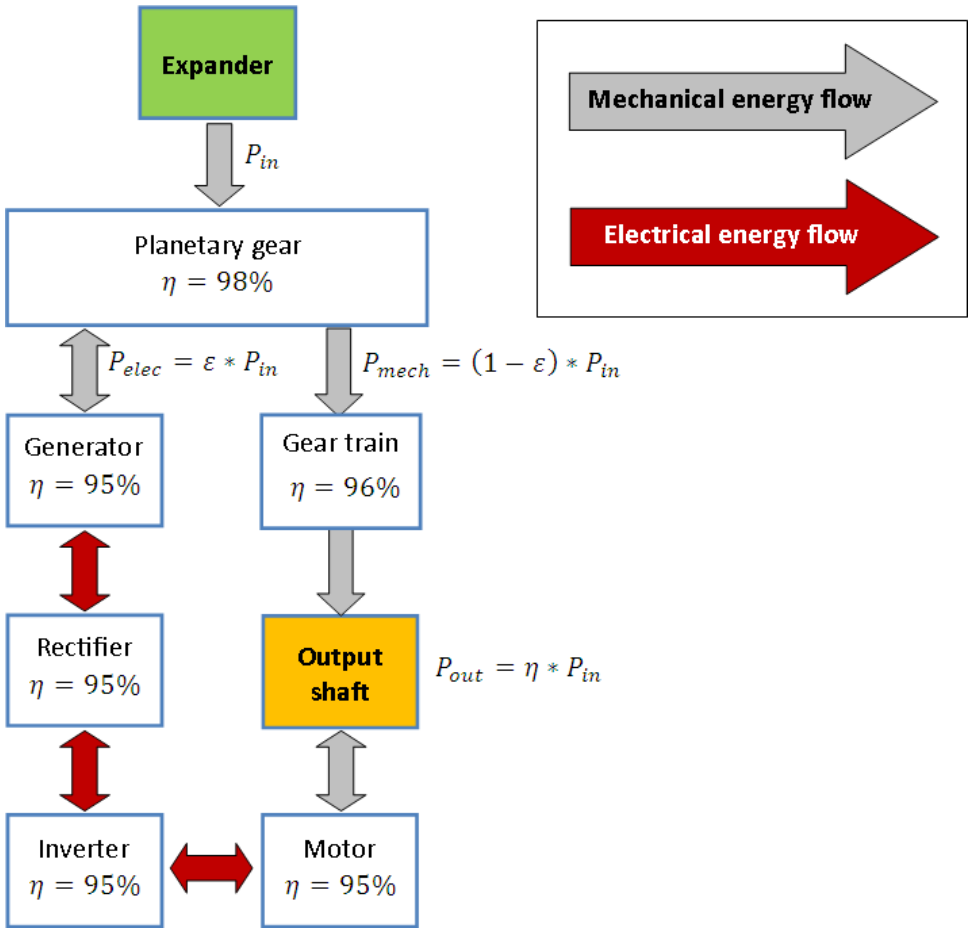

Figure 27: Input Power split configuration principle

A typical configuration for waste heat recovery applications would be to connect the expander shaft to the planet carrier, the mechanical branch to the ring gear and the electric branch to the sun gear as illustrated in Figure 28 and Figure 29 where C stands for planet carrier, S for sun gear and R for ring gear.

If the power transferred through the transmission is $P_{in} = P_{mech} + P_{elec}$, the power ratio is defined as $\varepsilon = \frac{P_{elec}}{P_{in}}$. The ratio value is not constrained and can be higher than one or lower than zero, it means that power can recirculate through the system and energy flow is not always in the same direction. Power recirculation has to be taken into account when dimensioning components since circulating power can excess input power.

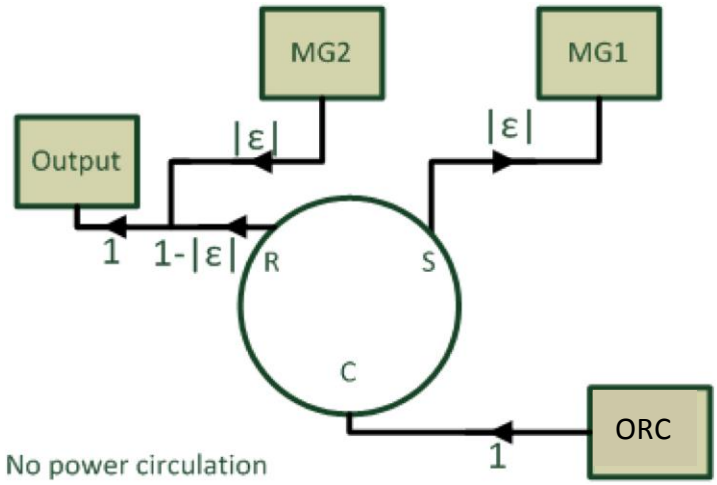

Figure 28: Power flow without power circulation [10]

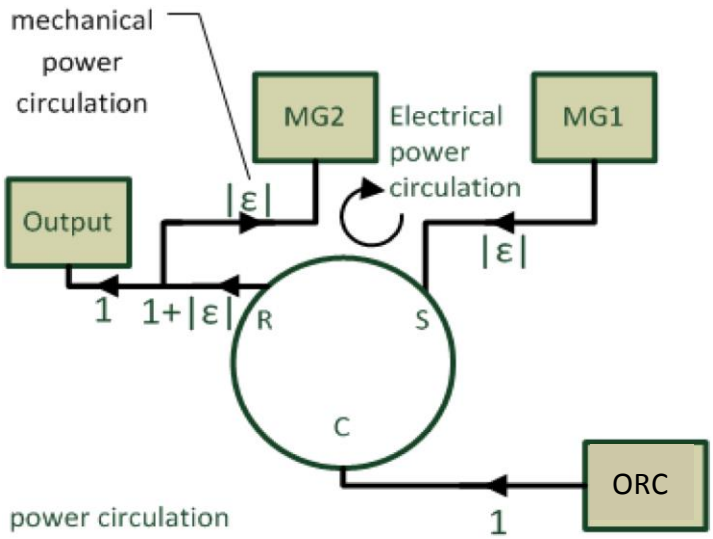

Figure 29: Power flow with power circulation [10]

The power ratio directly impacts the overall efficiency of the system which is:

$$\eta = (|\varepsilon| * \eta_{elec} + (1 - |\varepsilon|) * \eta_{mech}) * \eta_{planetary} \quad \textbf{3-3}$$

For the configuration shown in Figure 27 and according to the Willis equation, shaft speeds are linked as shown below:

$$\begin{cases} \omega_{exp} = \dfrac{S}{R+S} * \omega_{m1} + \dfrac{R}{R+S} * \omega_R \\ \omega_{eng} = \dfrac{1}{i_{gear}} * \omega_R \end{cases} \quad \textbf{3-4}$$

Similarly, torques can be computed as:

$$\begin{cases} T_{exp} = -\dfrac{R+S}{S} * T_{m1} \\ T_{eng} = \dfrac{R}{S} * i_{gear} * T_{m1} - i_{gear} * T_R \end{cases} \quad \textbf{3-5}$$

These equations combined with the speed ratio defined as $SR = \frac{\omega_{exp}}{\omega_{eng}}$ lead to the power ratio:

$$\varepsilon = \frac{R}{R+S} * i_{gear} * \frac{1}{SR} - 1 \quad \textbf{3-6}$$

Where R and S are respectively the radii of the ring and sun gears, subscripts exp, m1, R and eng respectively stand for expander, motor/generator 1, ring gear and engine and i_{gear} is the fixed gear ratio of the mechanical path.

The power ratio is thus a function of the speed ratio and gear ratios of planetary gears and reduction gears. So are generator and motor rotational speeds. For extensive explanations and demonstrations on power split devices and calculations, see [10].

Practically, the engine speed is imposed, so is the ring gear speed due to the fixed gear ratio in the mechanical branch. The speed ratio is thus controlled thanks to the electric branch and its frequency converter. As two speeds are now either imposed or controlled, the third planetary shaft (i.e. expander shaft) speed is also controlled and set to match the maximum efficiency expander operating point.

Typical efficiencies of electrical path and mechanical path of respectively 81% and 96%, in combination with planetary gear train efficiency of 98%, lead to an overall efficiency as depicted in Figure 30.

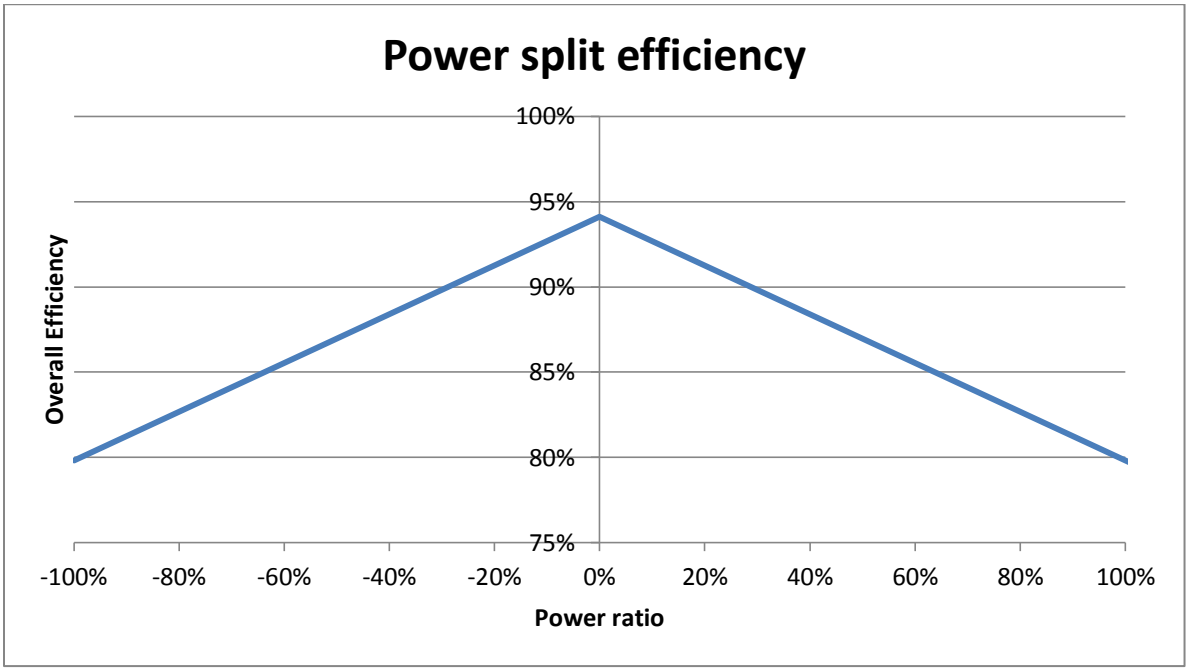

Figure 30: Typical input power split configuration efficiency

It then appears that the power ratio has to be minimized to achieve a higher overall efficiency, meaning that most of the power is transferred through the mechanical path.

The following results and curves depicted in Figure 31 and Figure 32 have been obtained for a ring gear radius of 10 cm and a sun gear diameter of 1.5 cm. These figures show power ratio and power split device efficiency as function of the speed ratio and rotational speed, torque and power for each power split device shaft.

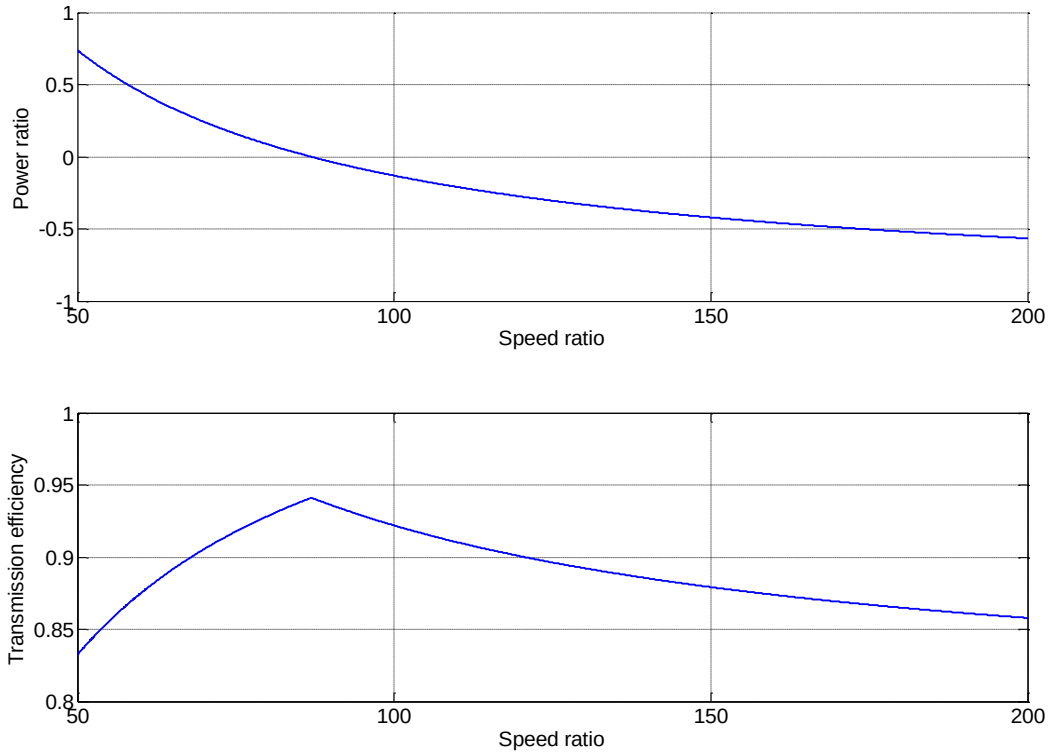

Figure 31: Power ratio and transmission efficiency

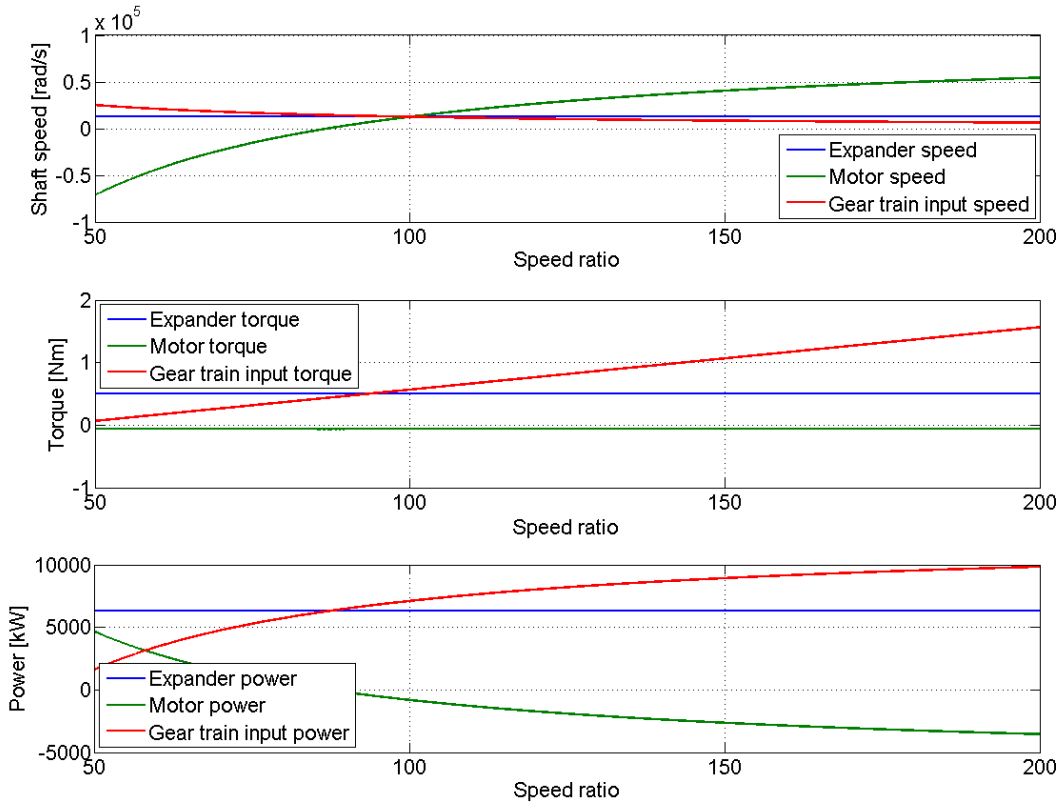

Figure 32: Rotational speeds, torques and powers of the different power split device shafts

Main power split system characteristics are shown in Table 8.

Table 8: Power split system characteristics

Input speed range	Up to 200000 rpm
Speed ratio range	Up to the ones achieved with fully mechanical or electrical transmissions
Transmission efficiency	83% to 94% depending on the speed ratio
Weight	Several kilograms
Size	No data found

3.6.1.2. Advantages

Thanks to its special features, this transmission has a continuously variable speed ratio and an overall efficiency higher than conventional CVT thanks to the high efficiency of the mechanical branch. This system offers the possibility to damp speed variations due to the variable speed ratio.

3.6.1.3. Drawbacks

As a drawback, this system is more complex and heavier than simpler transmissions. Depending on the dimensioning of the electric machines (i.e. the maximum power that can flow through the electric path), the system may not be able to uncouple input and output shafts since uncoupling involves that all the power should flow through the electric path and be dissipated in a resistor or stored in a battery.

3.7. Transmission overview summary

Table 9 shows a comparison matrix of all the systems previously described regarding all the criteria. Colors show how well a system meet a criterion (the greener, the better).

Table 9: System comparison matrix

Transmission type	Maximum speed ratio	Maximum input speed	Extra speed reduction required	Extra damping system required	Extra uncoupling system required	Variable speed ratio	Efficiency for input speed around 120000 rpm (turbine)	Efficiency for input speed around 6000 rpm (piston machine)	System complexity
Simple gear train	250000:1	Very high	No	Yes	Yes	No	94%	98%	Low
Planetary gear train	1000000:1	Very high	No	Yes	Yes	No	96%	98%	Low
Friction type CVT	6:1	12000 rpm	Yes	No	Yes	Yes	84%	86%	Moderate
Electric CVT	High	200000 rpm	No	No	No	Yes	81.5%	81.5%	High
Electric transmission with battery	High	200000 rpm	No	No	No	Yes	80%	80%	Very high
Power split transmission	High	200000 rpm	No	No	Yes/No	Yes	83% - 94%	84% - 96%	Very high

Chapter 4: Simulations

4.1. Simulated driving cycle and road conditions

The systems described and compared in Chapter 3: have been modeled and integrated to the complete vehicle model as explained in Appendix A: Transmission models descriptions. These completed drivelines will be compared to each other on two defined driving cycles regarding cycle average recovered power and fuel consumption.

The following transmission systems have been simulated and compared to the conventional system without energy recovery:

- Two planetary gear trains mounted in series configuration.
- A friction type CVT coupled together with a simple 2-stage gear train.
- An electric CVT.
- A micro-hybrid system: two electric motors and a short life battery.
- A power split system of input type coupled with both a simple 2-stage gear train one one side and an electric CVT on the other side.

4.1.1. Truck configuration

The truck configuration used during simulations is shown in Table 10.

Table 10: Truck configuration

Mass	40 tons
Engine	VT-NA MD13 500hp US10
Chassis	Long haul FH 4x2
Radiator	Confidential
Fan	Confidential
Cooling package configuration	Confidential
Transmission	AMT directdrive
Waste heat recovery expander	Turbine
Battery (for micro-hybrid configuration)	Li-ion 1.4 kWh

4.1.2. Sx 393 - Borås-Landvetter-Borås

The first driving cycle simulated is called Sx 393 – Borås-Landvetter-Borås. Its main characteristics are listed in Table 11 and more details regarding altitude, set speed and engine speed and torque distribution during the cycle are available in Figure 33 and Figure 34.

Table 11: Driving cycle Sx393 characteristics

Length	86.9 km
Maximum speed	85 km/h
Minimum altitude	20 m
Maximum altitude	152.35 m
Ambient temperature	18 °C

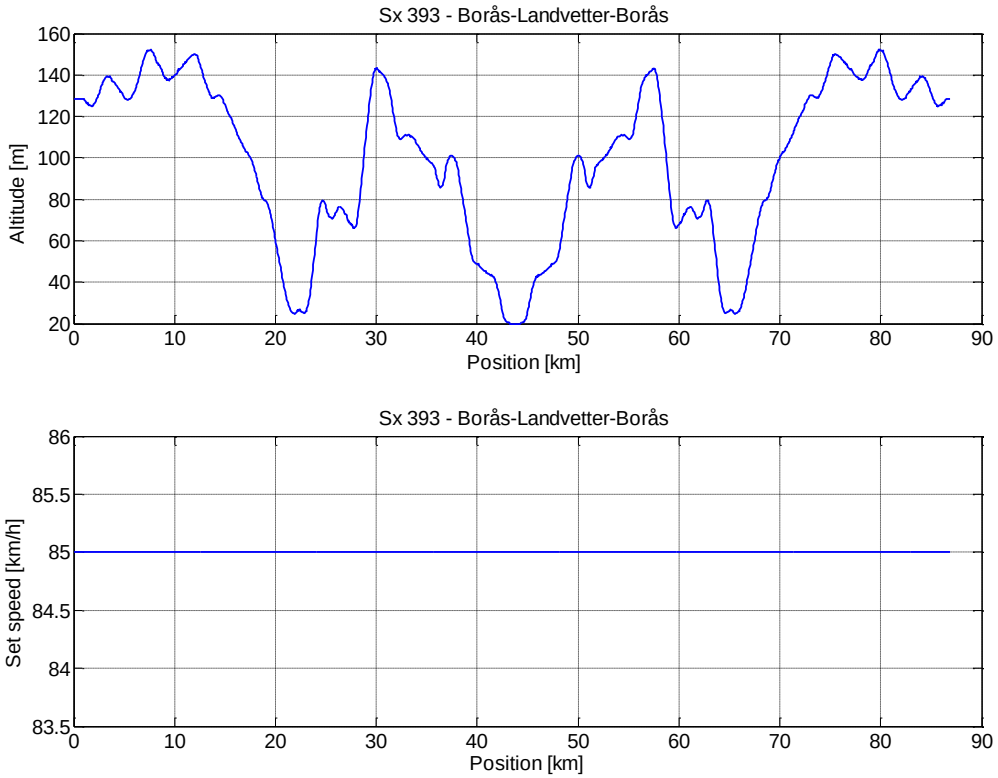

Figure 33: Sx 393 driving cycle altitude and set speed

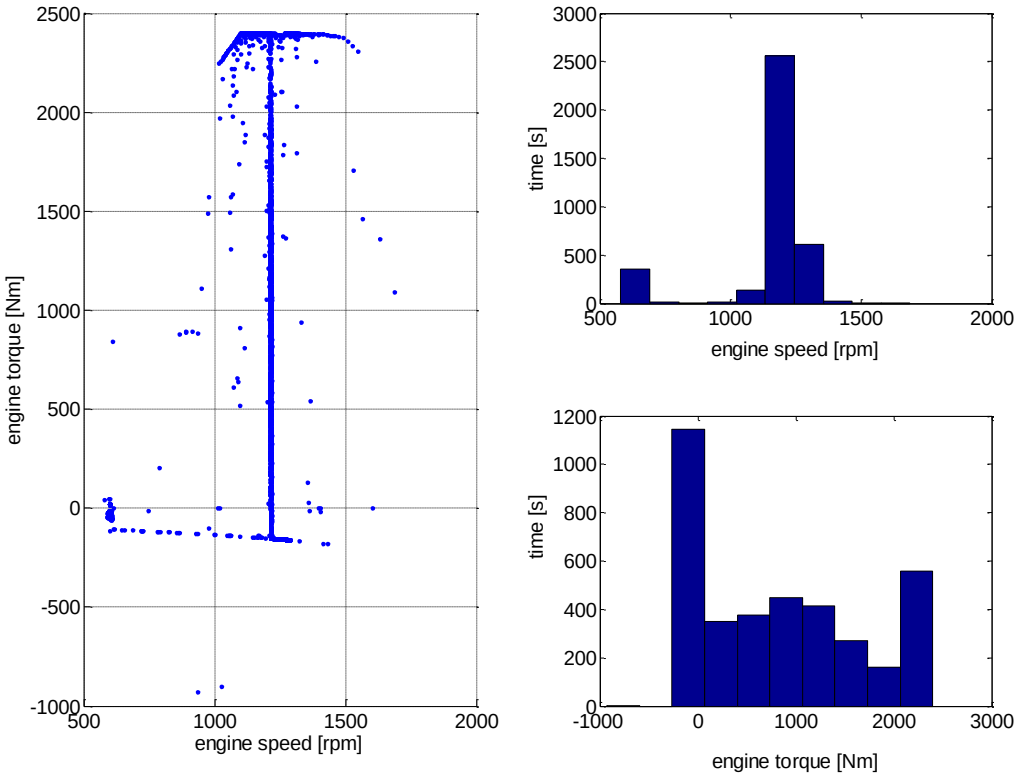

Figure 34: Engine torque and speed, Sx 393 driving cycle characteristics

4.1.3. Sx 145 - Germany predominantly flat

The second driving cycle simulated is called Sx 145 – Germany predominantly flat. Its main characteristics are listed in Table 12 and more details regarding altitude, set speed and engine speed and torque distribution during the cycle are available in Figure 35 and Figure 36.

Table 12: Driving cycle Sx145 characteristics

Length	546 km
Maximum speed	88 km/h
Minimum altitude	519 m
Maximum altitude	993.37 m
Ambient temperature	18 °C

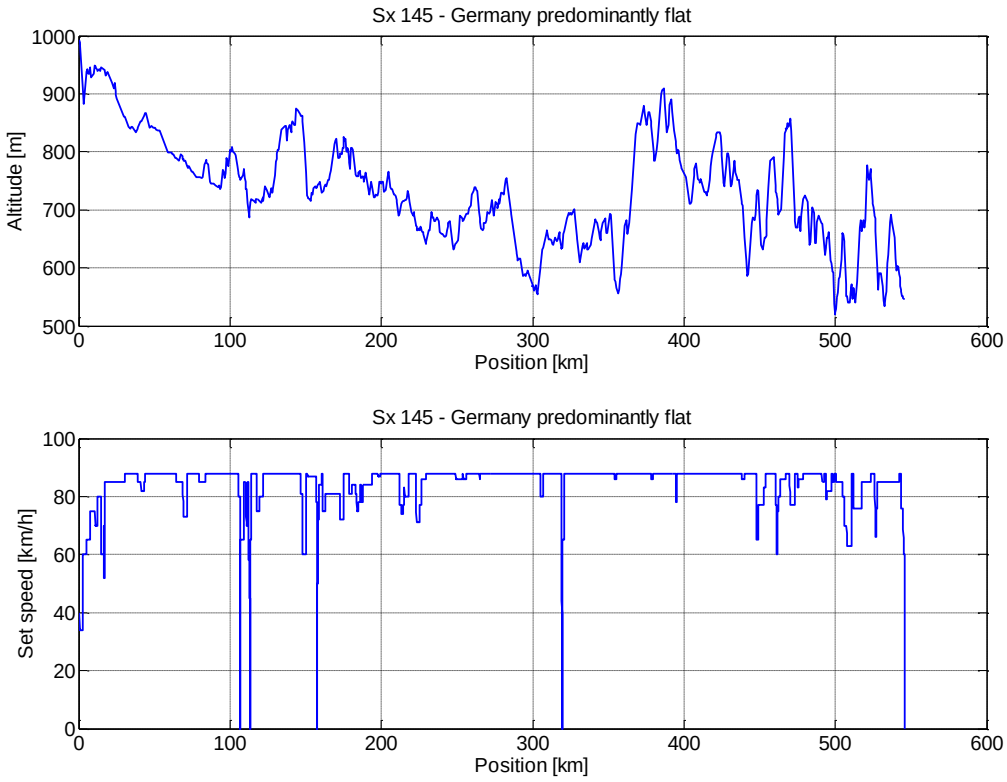

Figure 35: Sx 145 driving cycle altitude and set speed

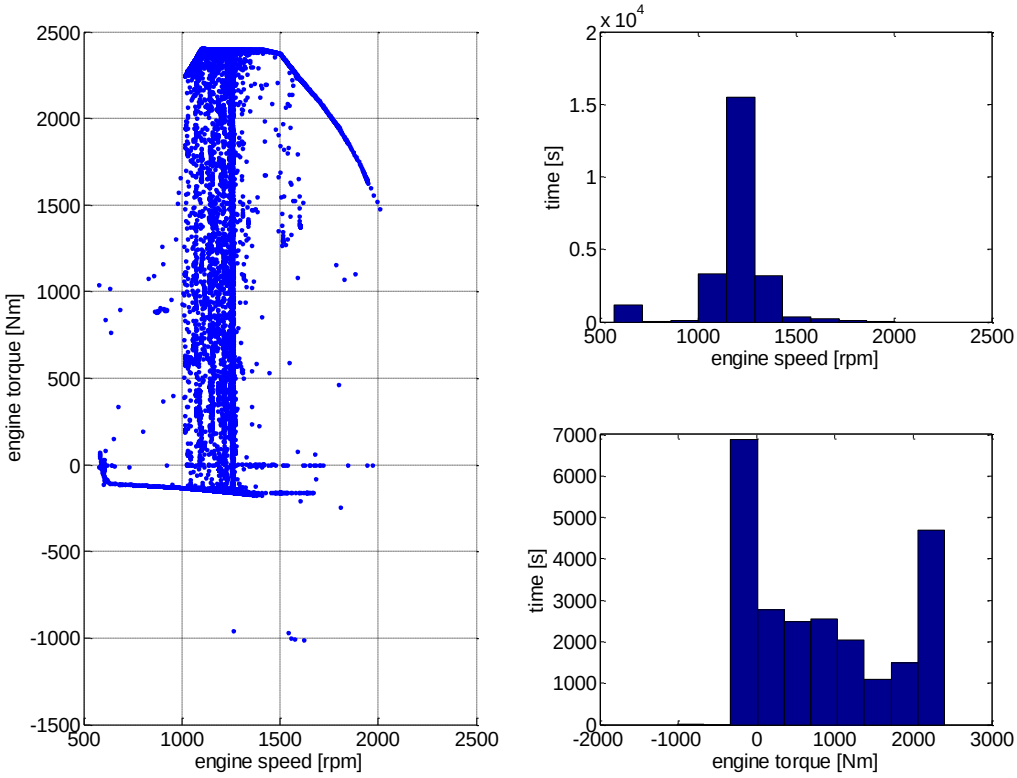

Figure 36: Engine torque and speed, Sx 145 driving cycle characteristics

Some general comments about the simulated driving cycles that arise:

- Both driving cycles are mostly highway driving at maximum permitted speed.
- Engine speed is most of the time around 1200 rpm.
- There are two peaks of engine torque, the biggest is engine brake torque, and the second is the maximum torque. During the rest of the cycle, engine torque is more or less uniformly spread on the whole engine torque range.

4.2. Simulation results

This section presents some results from simulations with different transmission systems and for both driving cycles. For each simulated driving cycle, average transmission losses and output powers are compared (see Figure 37 and Figure 38). Then fuel consumption and its relative reduction compared to the reference system (without waste heat recovery) are shown (see Figure 39 to Figure 42).

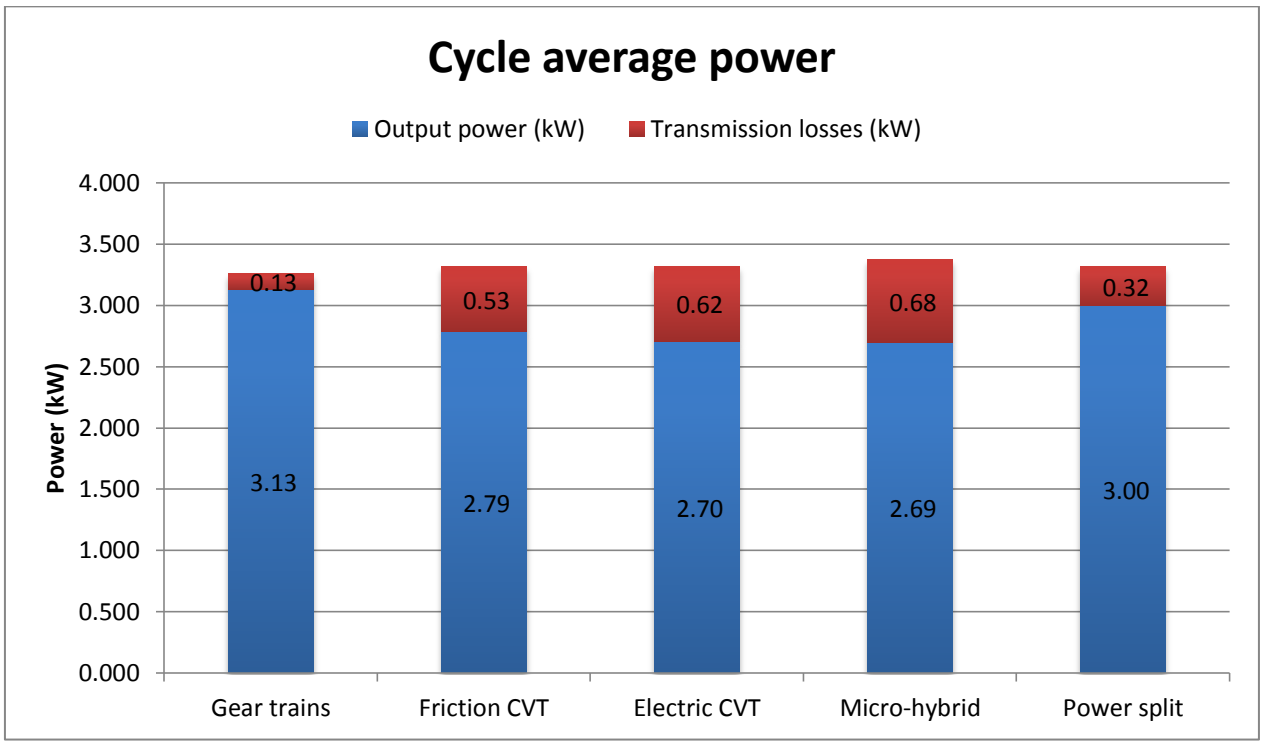

Figure 37: Sx 393 - Average power

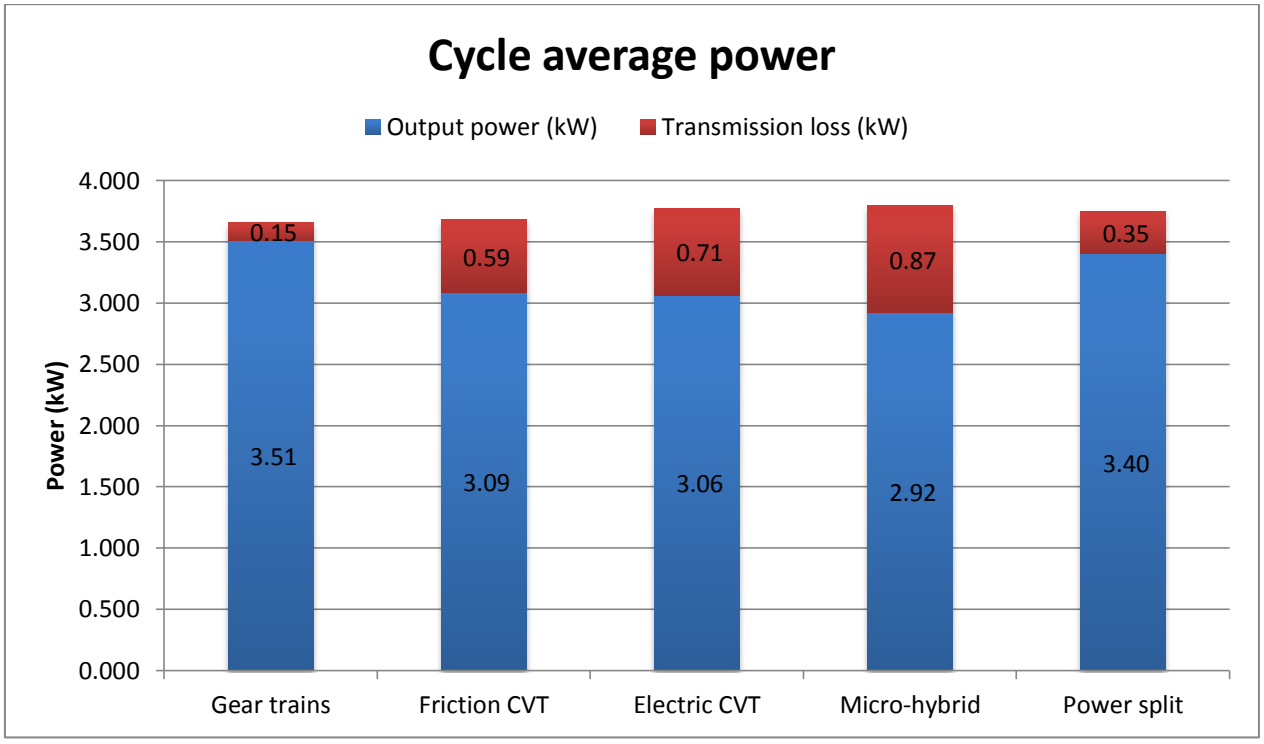

Figure 38: Sx 145 - Average power

Figure 37 and Figure 38 show that the micro-hybrid system enables to extract higher power in average on the cycle but it also has the largest transmission losses. Finally the highest output power[4] is obtained when gear trains are used as transmission system. Output power is then comprised between 3.1 and 3.5 kW.

[4] Net power after the transmission system

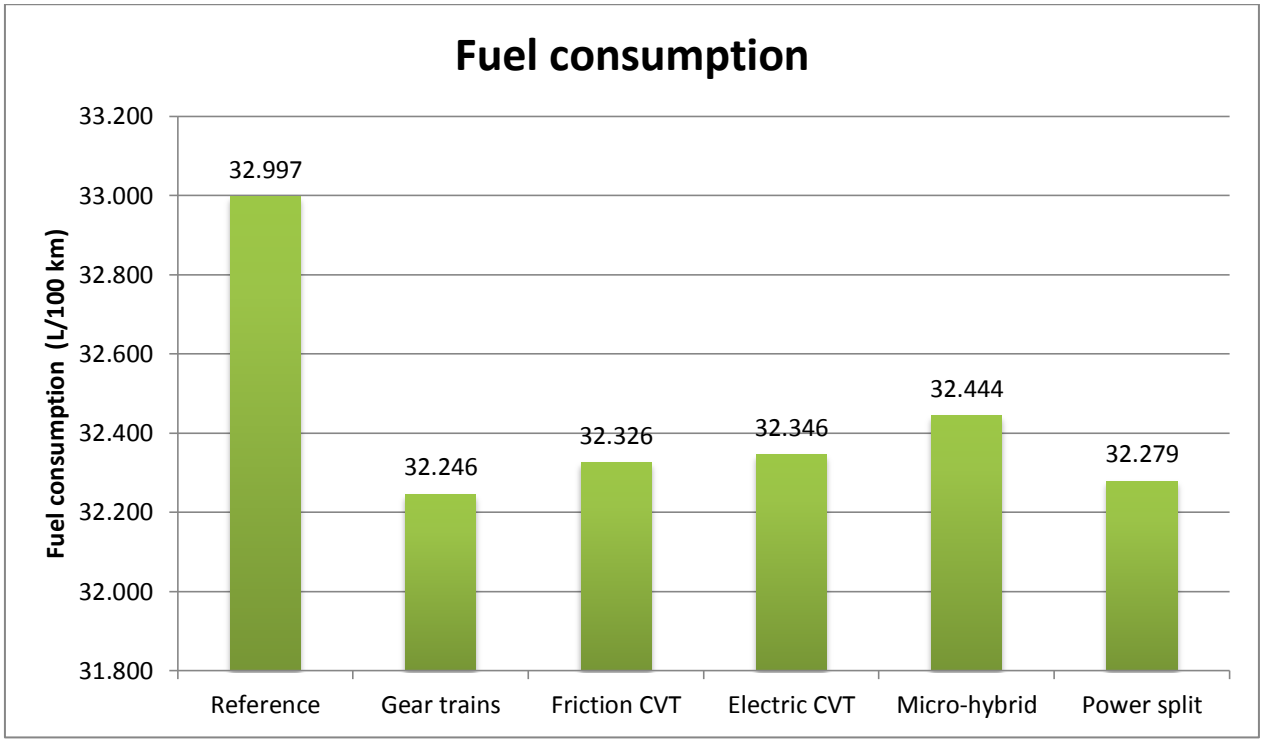

Figure 39: Sx 393 - Fuel consumption

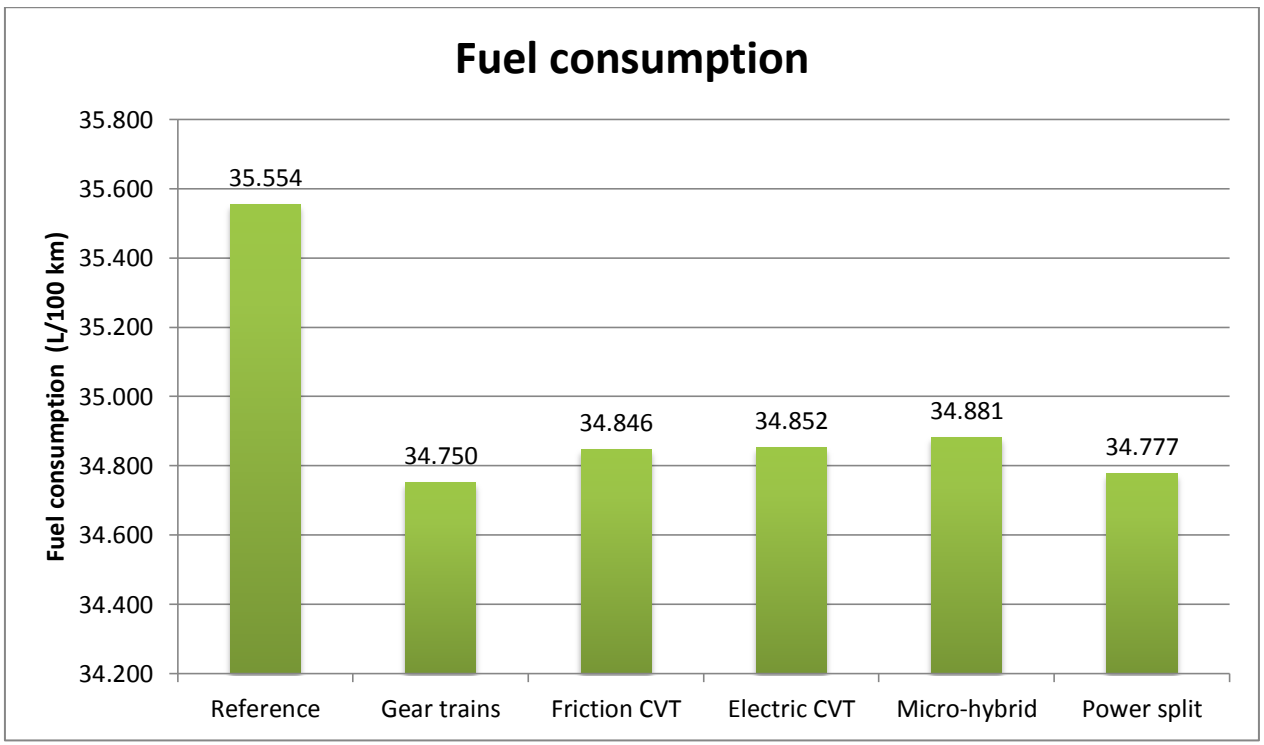

Figure 40: Sx 145 - Fuel consumption

As a consequence of different levels of output power, Figure 39 and Figure 40 show that the lower fuel consumption is got with a gear trains transmission. Up to 1L of fuel is then saved.

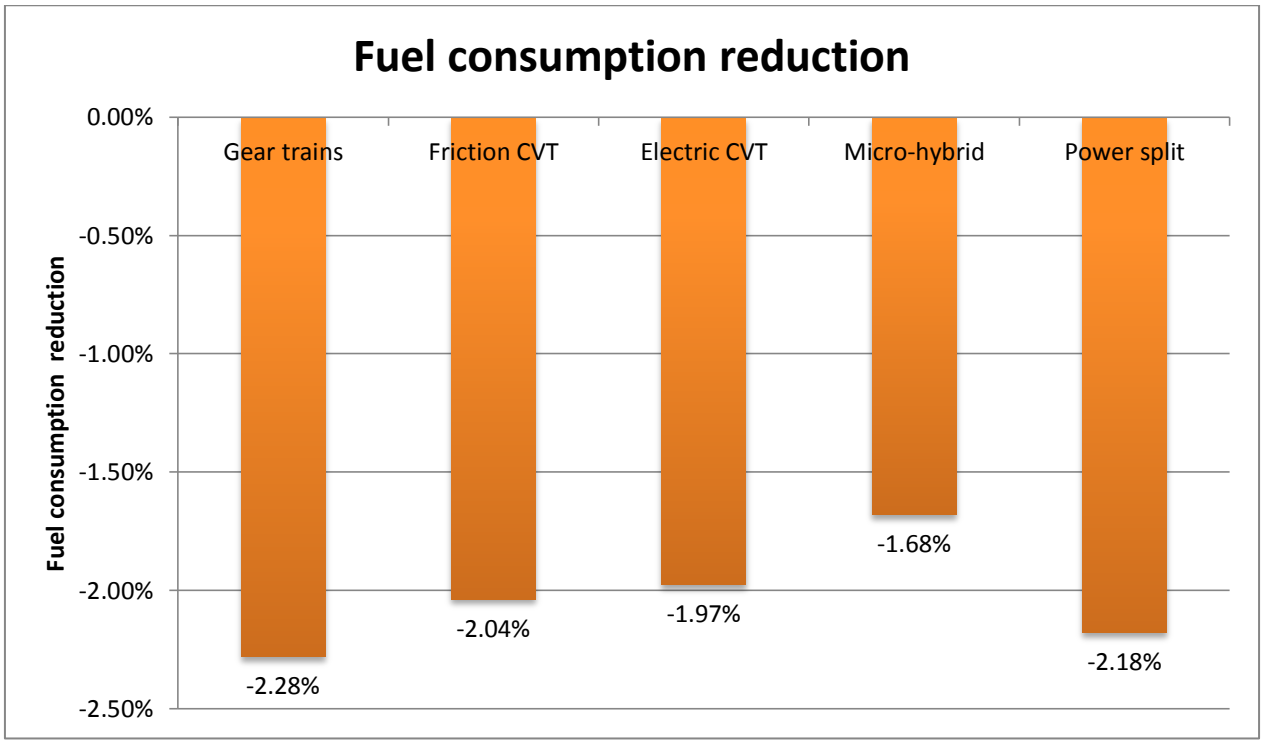

Figure 41: Sx 393 - Fuel consumption reduction

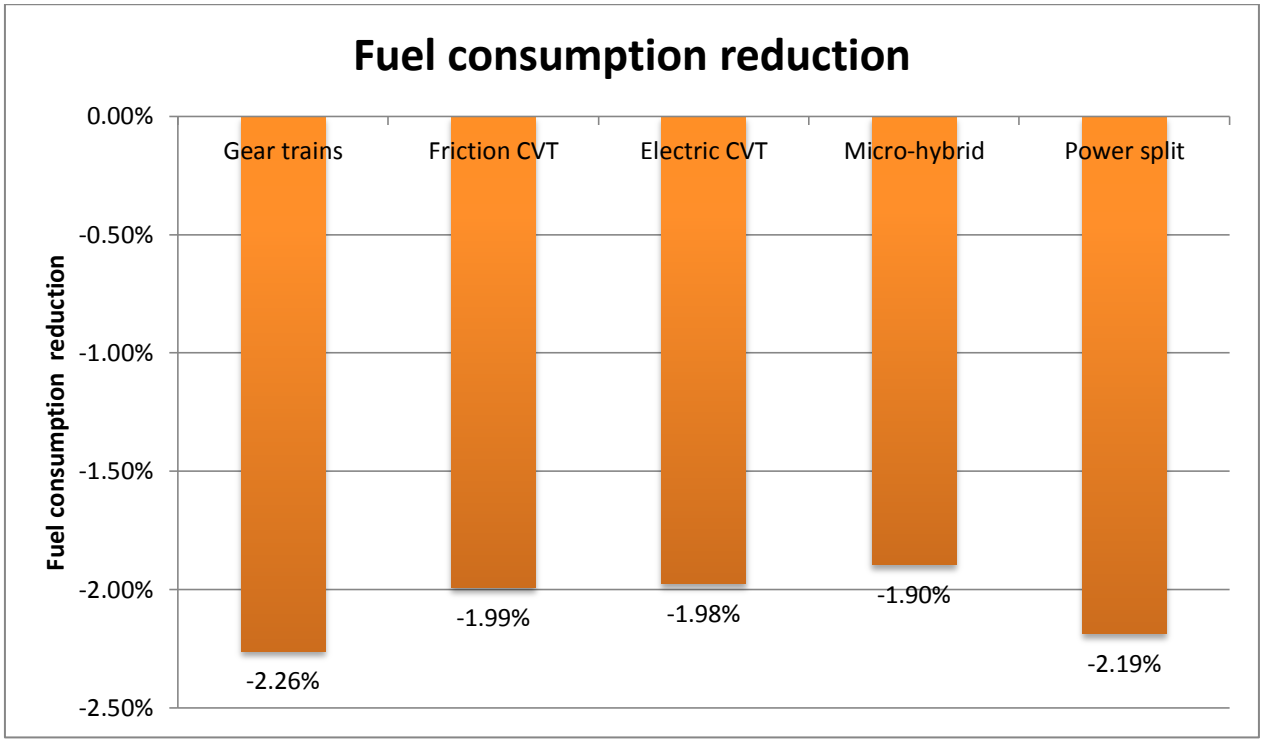

Figure 42: Sx 145 - Fuel consumption reduction

Fuel consumption reduction in percent is visible in Figure 41 and Figure 42. More than 2.25% of fuel is saved thanks to the gear trains transmission.

What can be highlighted from the results is that the average total recovered power from the turbine is higher when the speed ratio between expander and engine shafts is variable (see Figure 43). This phenomenon is due to the turbine operating in its most efficient conditions. The best configuration, in terms of average expander power, is when a battery is mounted since energy is more often recovered. On configurations without any storage device, the expander is bypassed when there is no need for additional power while braking for example. This is no longer valid if a storage device is mounted since energy can be stored when not needed. This results in a higher average expander power in the micro-hybrid configuration.

In spite of higher average expander powers on variable ratio configurations, average output powers are lower because of lower transmission efficiencies. Finally, the best choice, for these driving cycles, is to use planetary gear trains as they show the best results both concerning average output power and fuel consumption thanks to a very high efficiency compared to other solutions. Moreover, they are simple, quite compact and low cost.

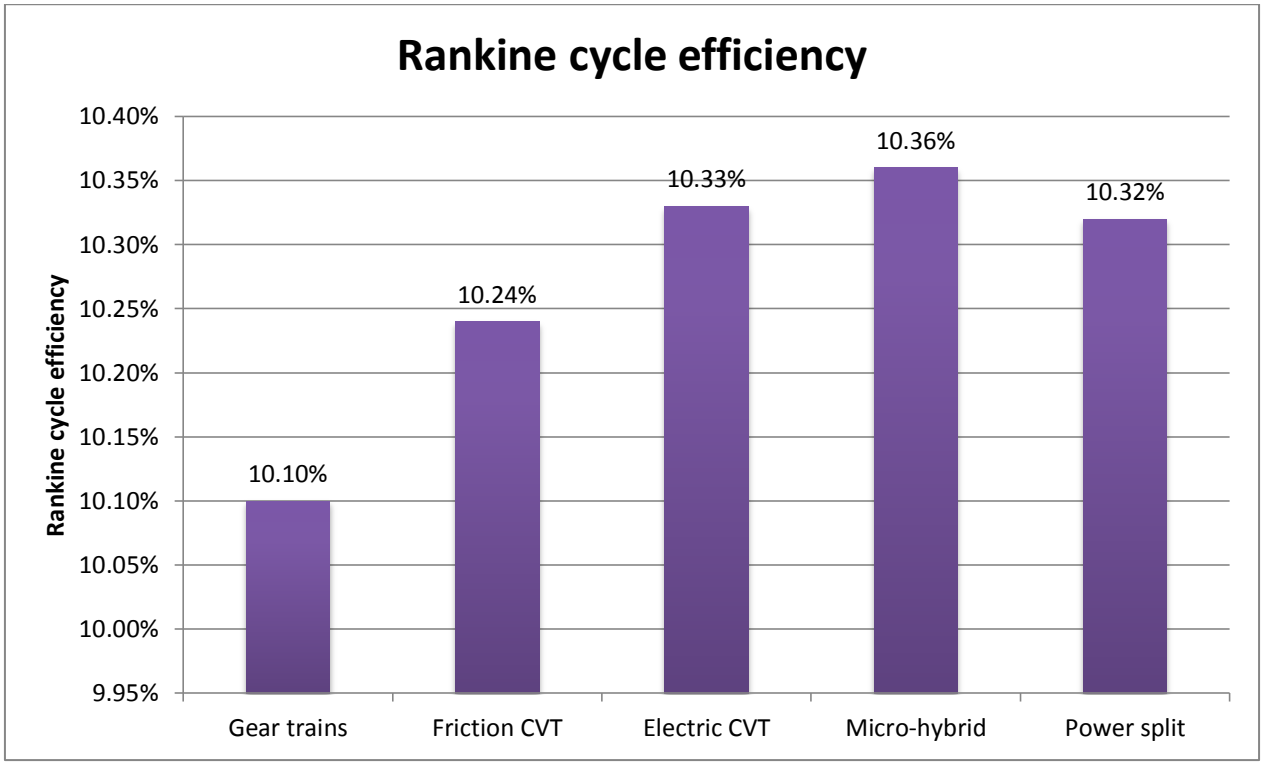

Figure 43: Sx 145 - Rankine cycle efficiency

Figure 44 shows that most of the solutions reduce the average engine efficiency. The engine and the gearbox are designed and controlled to operate at highest efficiency in normal driving conditions. On the one hand, the decrease in torque demand from the engine diverts the engine from its best operating point and leads to a lower efficiency. On the other hand, adding a battery increases the engine efficiency as one degree of freedom is added to the system and it is now possible to combine power sources to have them operating in their most efficient conditions.

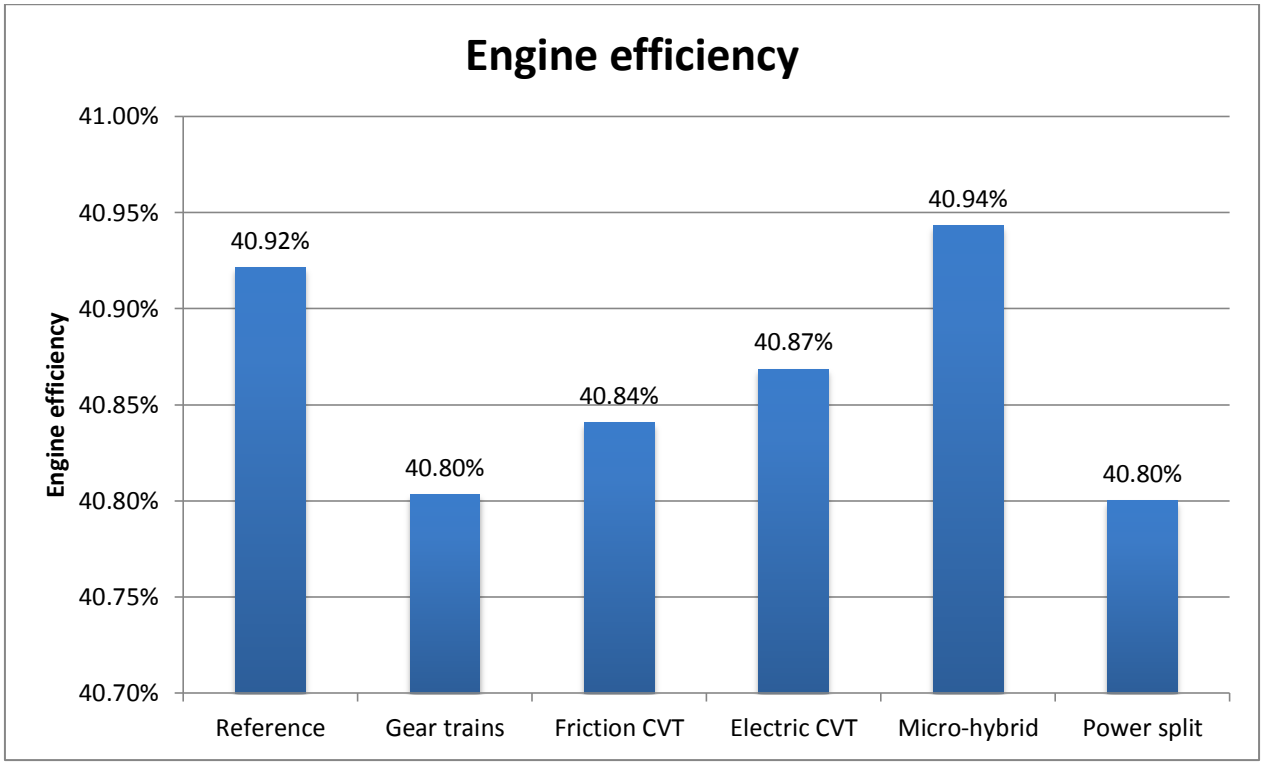

Figure 44: Sx 393 - Engine efficiency

Chapter 5: Conclusion

To conclude, the GSP model have been extended with the addition of a cooling system model offering three different cooling package architectures and a waste heat recovery model. Further work around the cooling system model should focus mainly on dynamic behavior and extensions to other engines.

Different types of transmission have been studied, compared and modeled with special attention to different characteristics: input power range, input speed range and speed ratio range for the application suitability, efficiency for the system performance and complexity, weight and size for future truck integration capacities. Cost evaluation might also help selecting the best solution even if it can be first assumed that cost is proportional to complexity and size.

Finally, simulations run on Sx 393 and Sx 145 driving cycles have shown that two planetary gear trains mounted in series configuration give the best results with and average gain in fuel consumption of 2.25%. It has to be noticed that these results were obtained on highway driving conditions with engine speeds about 1200 rpm most of the time (i.e. where the expander operates at maximum efficiency). Even if these cycles reflect the usual driving cycles for the kind of application considered in this report, further tests with harder road conditions should be carried out.

References

[1] Eurostat - Statistical Office of the European Communities, [Online]. Available: http://www.eea.europa.eu/. [Accessed June 2013].

[2] H. Teng, G. Regner and C. Cowland, "Waste heat recovery of heavy duty diesel engines by organic Rankine cycle part I: Hybrid energy system of Diesel and Rankine engines," SAE Technical paper 2007-01-0537, 2007.

[3] "Wikipedia - Rankine cycle," [Online]. Available: http://en.wikipedia.org/wiki/Rankine_cycle. [Accessed February 2013].

[4] R. Andersson, M. Cabanes, P. Templin, C. Gomes, B. Molimard, J. Emilsson and P. Dutal, "GSP Standards and Guidelines," Volvo, 2012.

[5] P. V. Gullberg, "PhD thesis: Optimisation of the Flow Process in Engine Bays - 3D Modelling of Cooling Airflow," Chalmers University of Technology, 2011.

[6] "The Transmission Bible," [Online]. Available: http://www.carbibles.com/transmission_bible.html. [Accessed May 2013].

[7] "How stuff works," [Online]. Available: http://auto.howstuffworks.com. [Accessed June 2013].

[8] "Electropaedia - Battery and Energy Technologies," [Online]. Available: http://www.mpoweruk.com/. [Accessed May 2013].

[9] "Wikipedia - Types of capacitor," [Online]. Available: http://en.wikipedia.org/wiki/Types_of_capacitor. [Accessed May 2013].

[10] T. Boehme, O. Metwally, B. Becker, N. Meinhardt, M. Rucht, H. Rabba and W. Drewelow, "A Simulation-Based Comparison of Different Power Split Configurations with Respect to the System Efficiency," SAE International 2012-01-0438, 2012.

[11] J. Bringhed and M. Åsbogård, "ER625291 - Flywheel-Kinetic Energy Recovery System evaluation for GTT applications," Volvo Powertrain Corporation, 2012.

[12] "High Speed Generator," e+a, [Online]. Available: http://www.highspeedgenerator.com/. [Accessed May 2013].

[13] B. Bonsen, "PhD thesis: Efficiency optimization of the push-belt CVT by variator slip control,"

Eindhoven University of Technology, 2006.

[14] D. Clenet, "Cahier Technique n°208: Démarreurs et variateurs de vitesse électroniques," Schneider Electric, 2003.

[15] C. De Metsenaere, "Survey into CVT slip control potential using MATLAB Simulink simulation," Eindhoven Technical University, DCT-2004-76, 2004.

[16] N. Espinosa, "PhD thesis: Contribution to the study of waste heat recovery systems on commercial truck Diesel engines," Institut national polytechnique de Lorraine & Université de Liège, 2011.

[17] R. Le Borzec, "Réducteurs de vitesse à engrenages," Techniques de l'Ingénieur - B5640, 1992.

[18] K. T. Renius and R. Resch, "Continuously Variable Tractor Transmissions," ASAE Distinguished Lecture No. 29, pp. 1-37., 2005.

[19] Y. Rothenbühler, "PhD thesis: New Slip Synthesis and Theoretical Approach of CVT Slip Control," Ecole Polytechnique Fédérale de Lausanne - 4337, 2009.

[20] P. Venet, "Les supercondensateurs - Conference," Laboratoire Ampère, Villeurbanne, 2012.

Appendices

Appendix A: Transmission models descriptions

I. Gear trains

The model works for both simple gear trains and planetary gear trains.

It takes, as input parameters, the number of stages, stage speed ratio (identical for all stages) and stage efficiency. Then torques and speeds are computed from input values.

Simulations were made with a fixed speed ratio of 100 and an overall efficiency of 0.96.

II. Friction CVT

The model takes the desired expander speed (usually where the expander efficiency is the highest) as input parameter and computes the requested speed ratio. This speed ratio cannot exceed 1:3 and 3:1 due to physical limitations and a rate limit is also applied.

Torques and speeds are computed based on the speed ratio and the efficiency given as input parameter.

Transmission efficiency was set to 0.875 for simulations.

III. Electric CVT

The model is composed of two electric motors/generators that were already modeled in GSP. These two models were slightly modified in terms of power demand. The generator electric demand is the expander output power and the motor mechanic power demand is the generator output power.

A frequency converter is inserted between the two electric motors to vary the current frequency so that the expander operates at its highest efficiency point.

For simulations, each component efficiency was set to 0.95 and electric motors maximum speeds, torques and powers was defined to match the overall system requirements with some margins.

IV. Micro-hybrid system

The model layout is the same as for the electric CVT except that a battery (already modeled in the GSP library) is inserted between the generator and the frequency converter. Electric power demand from the generator is the expander output power.

An energy management strategy was established to control the power demand from the electric motor as well as to prevent the battery to self-deteriorate keeping the state of charge level between its nominal boundaries. The strategy is shown in Figure 45. Three choices are possible:

- The battery can be loaded: in that case, there is no energy going out of the battery meaning that the motor outputs nothing.
- Energy can be transferred: it means that there is as much energy flowing in and out of the battery. The power demand from the electric motor is thus the expander output power.
- The battery can be emptied: in that case, the power demand from the motor is its maximum power.

The parameter $\ddot{m}_{threshold}$ was set to 10 kg/s².

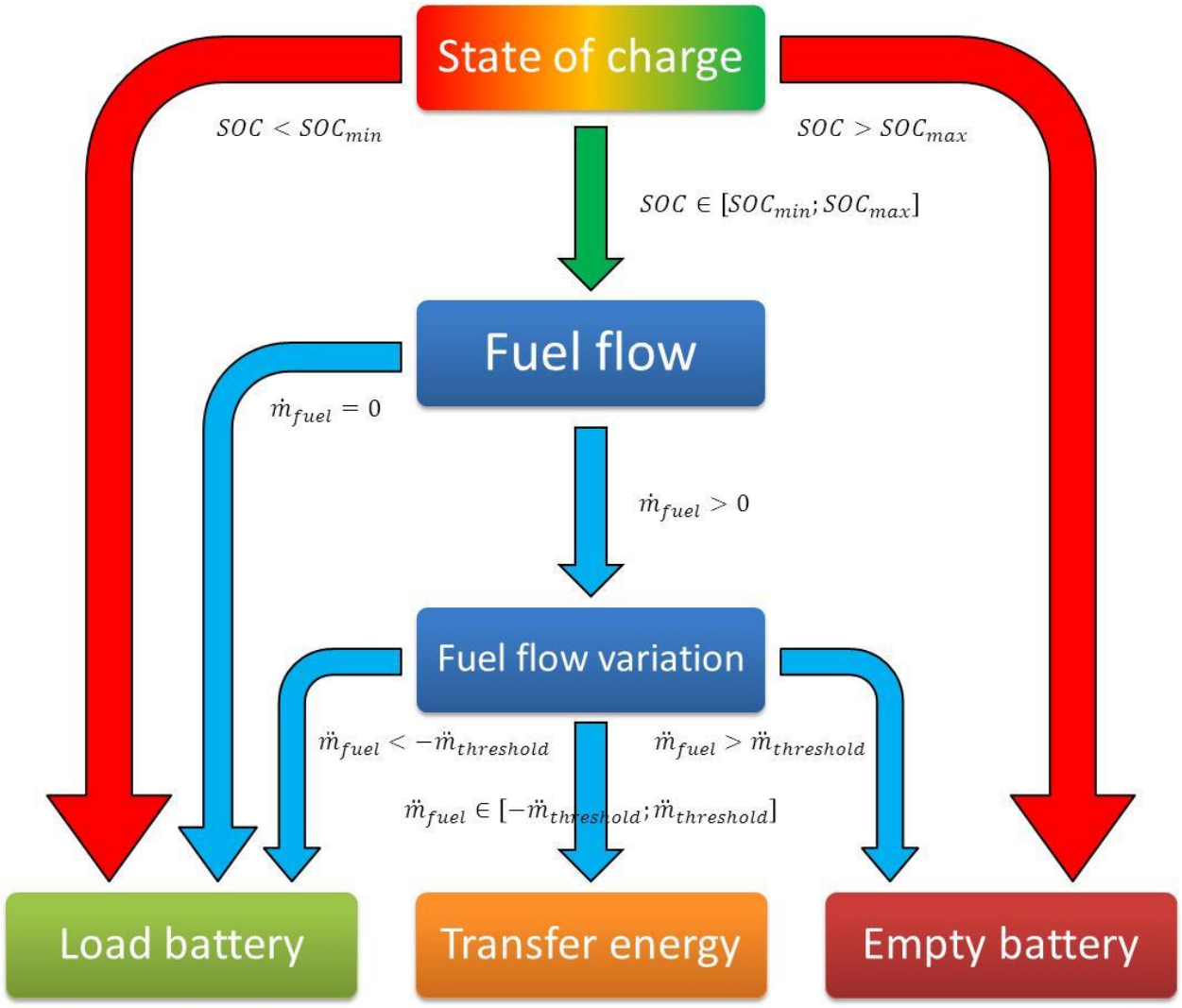

Figure 45: Micro-hybrid system energy management strategy

V. Power split system

The power split model computes the speed ratio between expander and output shafts and then derives the power ratio. Then torques and speeds for both branches are computed given a set of planetary gear geometric parameters. Then the model feeds a gear train model block and a CVT-like model that represents the electric branch.

The planetary gear efficiency was 98%, the gear train efficiency was 96% and the electric branch efficiency was 81%. The fixed speed ratio of mechanical branch was set to 100. The ring gear radius of the planetary gear was 0.1m and the sun gear radius was 0.015m.